Chemosphere 308 (2022) 136110

Contents lists available at ScienceDirect

Chemosphere

journal homepage: www.elsevier.com/locate/chemosphere

Proteomics reveals multiple effects of titanium dioxide and silver nanoparticles in the metabolism of turbot, *Scophthalmus maximus*

Mário J. Araújo [a,*], Maria L. Sousa [a], Elza Fonseca [a], Aldo Barreiro Felpeto [a], José Carlos Martins [a], María Vázquez [b], Natalia Mallo [b], Laura Rodriguez-Lorenzo [c], Monica Quarato [c], Ivone Pinheiro [c], Maria V. Turkina [d], Juan José López-Mayán [e], Elena Peña-Vázquez [e], María Carmen Barciela-Alonso [e], Miguel Spuch-Calvar [f], Miguel Oliveira [g], Pilar Bermejo-Barrera [e], Santiago Cabaleiro [b], Begoña Espiña [c], Vitor Vasconcelos [a,h], Alexandre Campos [a]

[a] *CIIMAR - Interdisciplinary Centre of Marine and Environmental Research, Terminal de Cruzeiros do Porto de Leixões, Av. General Norton de Matos s/n, 4450-208, Matosinhos, Portugal*
[b] *CETGA - Cluster de la Acuicultura de Galicia, 15965, Ribeira, Galicia, A Coruña, Spain*
[c] *INL - International Iberian Nanotechnology Laboratory, Avda. Mestre José Veiga s/n, Braga, Portugal*
[d] *Department of Biomedical and Clinical Sciences, Faculty of Medicine and Clinical Sciences, Linköping University, 581 83, Linköping, Sweden*
[e] *GETEE - Trace Element, Spectroscopy and Speciation Group, Institute of Materials iMATUS, Department of Analytical Chemistry, Nutrition and Bromatology, Faculty of Chemistry, Universidade de Santiago de Compostela, Avenida das Ciencias, s/n., 15782, Santiago de Compostela, Spain*
[f] *TeamNanoTech / Magnetic Materials Group, CINBIO, Universidade de Vigo - Campus Universitario Lagoas Marcosende, 36310, Vigo, Spain*
[g] *Centre for Environmental and Marine Studies (CESAM), University of Aveiro, 3810-193, Aveiro, Portugal*
[h] *Biology Department, Faculty of Sciences, University of Porto, Rua do Campo Alegre, s/n, 4169-007, Porto, Portugal*

HIGHLIGHTS

- TiO_2 and Ag NPs induced histological and proteomic alterations, mainly in liver.
- Titanium and silver accumulated in turbot liver.
- TiO_2 and Ag NPs affected energy/lipid metabolism.
- Ag NPs also altered ribosome and protein biosynthesis related processes and others.
- The proteomic study provided candidate biomarkers for NPs exposure.

GRAPHICAL ABSTRACT

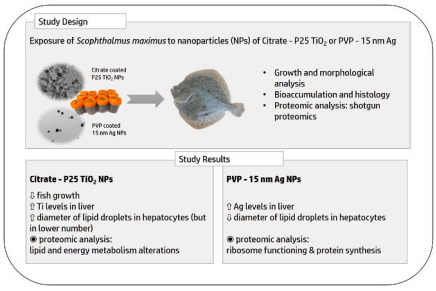

ARTICLE INFO

Handling Editor: James Lazorchak

Keywords:
Ecotoxicology
Flatfish
Shotgun proteomic

ABSTRACT

Titanium dioxide (TiO_2) and silver (Ag) NPs are among the most used engineered inorganic nanoparticles (NPs); however, their potential effects to marine demersal fish species, are not fully understood. Therefore, this study aimed to assess the proteomic alterations induced by sub-lethal concentrations citrate-coated 25 nm ("P25") TiO_2 or polyvinylpyrrolidone (PVP) coated 15 nm Ag NPs to turbot, *Scophthalmus maximus*. Juvenile fish were exposed to the NPs through daily feeding for 14 days. The tested concentrations were 0, 0.75 or 1.5 mg of each NPs per kg

* Corresponding author.
E-mail address: mario.araujo@ciimar.up.pt (M.J. Araújo).

https://doi.org/10.1016/j.chemosphere.2022.136110
Received 4 June 2022; Received in revised form 1 August 2022; Accepted 16 August 2022
Available online 22 August 2022

Differential protein expression
Molecular physiology
Organ specific response

of fish per day. The determination of NPs, Titanium and Ag levels (sp-ICP-MS/ICP-MS) and histological alterations (Transmission Electron Microscopy) supported proteomic analysis performed in the liver and kidney. Proteomic sample preparation procedure (SP3) was followed by LC-MS/MS. Label-free MS quantification methods were employed to assess differences in protein expression. Functional analysis was performed using STRING web-tool. KEGG Gene Ontology suggested terms were discussed and potential biomarkers of exposure were proposed. Overall, data shows that liver accumulated more elements than kidney, presented more histological alterations (lipid droplets counts and size) and proteomic alterations. The Differentially Expressed Proteins (DEPs) were higher in Ag NPs trial. The functional analysis revealed that both NPs caused enrichment of proteins related to generic processes (metabolic pathways). Ag NPs also affected protein synthesis and nucleic acid transcription, among other processes. Proteins related to thyroid hormone transport (*Serpina7*) and calcium ion binding (*FAT2*) were suggested as biomarkers of TiO_2 NPs in liver. For Ag NPs, in kidney (and at a lower degree in liver) proteins related with metabolic activity, metabolism of exogenous substances and oxidative stress (e.g.: NADH dehydrogenase and Cytochrome P450) were suggested as potential biomarkers. Data suggests adverse effects in turbot after medium/long-term exposures and the need for additional studies to validate specific biological applications of these NPs.

1. Introduction

Nanoparticles (NPs) refer to materials having at least one dimension with a size below 100 nm (Koo, 2006; Khalil et al., 2011). These materials properties are different from the ionic forms or other forms of the elements (e.g.: mechanical, chemical, catalytic or optical properties) which makes them relevant for a wide range of industrial and biomedical applications. As a result of its use, many NPs will end in aquatic compartments (water and sediments), having the potential to affect aquatic organisms, including species with commercial interest (Bundschuh et al., 2018; Giese et al., 2018; Biswas and Sarkar, 2019; Madanayake et al., 2022).

The safety of nanoparticles is controversial since some NPs are categorized as biologically inert (Umair et al., 2016; Kose et al., 2020), however, there is increasing concern about their toxicity under specific conditions and there is a need to perform more studies considering their different routes of exposure, addressing effects and uptake by aquatic organisms. A range of effects of NPs including oxidative stress, cellular pathologies consistent with tumour formation, organ-specific ion--regulatory disturbances, and vascular injury, among others, have already been reported (Handy et al., 2008; Powers et al., 2011). From a toxicological point of view, distinct forms of NPs should not be considered identical materials, since different biological responses have been described. It has been shown that size, shape, surface charge, type of functionalization processes (e.g.: by addition of coatings and radiation) or core structure will endow materials with different bioactivity (e.g.: Chen et al., 2014; Powers et al., 2011; Helmlinger et al., 2016, Kędziora et al., 2018; Chow, 2021). It is established that there is a high level of interaction between proteins and NPs, leading to the nanoparticle-protein-corona formation that facilitates cellular uptake, inflammation and accumulation, among other interactions (Saptarshi et al., 2013). Therefore, understanding the roles and the interaction of NPs with proteins (both chemical and "functional" alteration) is a research need (Lynch and Dawson, 2008; Amde et al., 2017).

Titanium dioxide (TiO_2) NPs and silver (Ag) NPs are amongst the most commonly used and studied engineered inorganic NPs. TiO_2 NPs are used in personal care products (PCP), mainly as UV filters in sunscreens, but also in paints and coatings (Jovanović et al., 2015; Sharma et al., 2019; Musial et al., 2020). Although TiO_2 NPs have been as well used as a food additive, their integration in food products is becoming more restricted due to safety concerns (Bischoff et al., 2020). Since 2006 International Agency for Research on Cancer (IARC) has been showing the risks of food additive E171, which is composed of up to 40% of TiO_2 NPs, as a possible carcinogen for humans (IARC Working, 2010). Therefore, this additive was banned in France (ANSES, 2019) and the European Food Safety Authority (EFSA) classified E171 as no longer safe for consumption (EFSA, 2021). The unintended release of these NPs to the environment is also of concern since they may affect aquatic organisms (Skocaj et al., 2011; Asztemborska et al., 2018). The acute or chronic uptake and ingestion of TiO_2 NPs (even at low concentrations) induce a wide range of effects in organisms. The exposure of mice to TiO_2 NPs seems to result in effects on the microbiome proteome in multiple pathways, which may lead to the appearance of chronic diseases (Cao et al., 2020). Several studies reveal that TiO_2 NPs exposure can result in histological changes and a series of harmful effects, including genotoxic and potentially cytotoxic in fish (e.g.: Vignardi et al., 2015). In addition, previous studies reported that exposure to TiO_2 NPs enhances the deleterious effects caused by other stressors, including vulnerability to bacterial outbreaks (Jovanović et al., 2015).

In addition to their use in electronic devices and PCP (Janković and Plata, 2019), Ag NPs are also of foremost importance for several fields of biomedical science, since they are known for their antibacterial, antiviral, antifungal action (Yin et al., 2020). Its continuing ion release ability allows an increase in the antimicrobial efficacy and bioavailability of silver. Concerns related with an increase in microbial resistance are also arising, resulting from the ubiquitous presence of Ag NPs in the environment. The Ag NPs are also used as a food additive and lack of toxicological information has been referred (EFSA, 2016). A range of effects can result from Ag NPs exposure, including cytotoxicity, oxidative damage, alterations in the regulation of enzymes responsible for free radical scavenging, disrupted processes of storing, detoxification and metabolism of metals and altered expression of genes involved in apoptotic pathways; however, the mechanisms of action are still not well understood (Stensberg et al., 2011; Aerle et al., 2013; Austin et al., 2014; Lee et al., 2015; Ivanova et al., 2018; Ferdous & Nemmar 2020; Yin et al., 2020).

Difficulties arise from sampling, characterization and quantification of NPs in natural environments (Aznar et al., 2017; Dedman et al., 2021; Tou et al., 2021), Nevertheless, their presence/absence is often represented in terms of number per volume and the total concentrations of their corresponding elements is also relevant. The maximum concentrations of total titanium or silver are below 50 $\mu g\ L^{-1}$ in aquatic environments and result mainly by the proximity to highly populated areas (Tovar-Sanchez et al., 2013; Aznar et al., 2017; Liu and Hurt, 2010; Dedman et al., 2021). Their detection is also frequent in sewage and in sediments where NPs can reach millions of parts/mg (Bäuerlein et al., 2017; Tou et al., 2021). Therefore, demersal fish are continuously in contact with TiO_2 or Ag NPs during their life and a high trophic exposure risk also exists (Wang et al., 2014; Silva et al., 2022). Alternatively, aquaculture-farmed species may be in contact with NPs through feeds enhancers or pharmaceutical products (Khosravi-Katuli et al., 2017; Shah et al., 2019).

Proteomics is commonly referred to as the large-scale study of proteins and allows identifying proteins related with alterations in multiple biological functions and molecular pathways in living organisms. Proteomics has been proven as a valuable research tool to understand alterations of mechanisms that may lead to the appearance of diseases, including chronic conditions and the discovery of new biomarkers (e.g.:

Wiśniewski et al., 2011; Zhang et al., 2011; Campos et al., 2012; Li and Chan, 2014; Chan et al., 2016; Causey et al., 2018; among others). Proteomics can thus be useful in a wide range of applied fields of biology, such as toxicology, food safety and aquaculture (Campos et al., 2016; Rodrigues et al., 2016, 2017; Felice and Parolini, 2020; Martins et al., 2020).

Therefore, in this work, we aim to study the effects of two common NPs on turbot, *Scophthalmus maximus*, since this marine flatfish species is one of the most valuable fish captured in the wild and is also of high economic importance in aquaculture, being produced in Europe, China and Chile (EUMOFA, 2018; Food and Agriculture Organization and Gonzalez Serrano, 2022). To this end, we studied the alterations in liver and kidney proteomes in response to citrate-coated 25 nm ("P25") TiO_2 and polyvinylpyrrolidone (PVP) coated 15 nm Ag NPs after 14 days of exposure through feeding. In addition, new biomarkers for studying the effects of NPs exposure are also suggested.

2. Material and methods

2.1. Nanoparticles characterization

Commercially available P25 TiO_2 NPs and 15 nm Ag NPs were supplied by Sigma-Aldrich (product code: 718467) and SSNAno (Houston, TX, USA; product code: 0127SH), respectively. Characterization was performed at the International Iberian Nanotechnology Laboratory (INL, Braga, Portugal, Supplementary Material 1, SM1).

Prior to its use, TiO_2 P25 NPs have been stabilised by trisodium citrate dihydrate (Sigma-Aldrich) by dispersing them at a weight ratio of TiO_2:citrate 1:0.8, *wt*:*wt* using an ultrasonic probe (for a total of 40 min, with 30 s pulse-on/5 s pulse-off, 70% amplitude). Silver powder instead presents a composition of 25% *wt* of silver and 75% *wt* polyvinylpyrrolidone (PVP). 1 g L^{-1} stock suspension was prepared for both NPs by dispersing the particles in ultrapure water and stored at 4 °C until further use.

The colloidal stability of the NPs in ultrapure water and artificial seawater (35 ppm salinity) was analysed by dynamic light scattering and zeta potential. Dispersions in both media with a concentration of 50 mg L^{-1} were prepared to dilute the stock solution (e.g. 500 μL of 1 g L^{-1} stock in 9500 μL of seawater). The characterization by dynamic light scattering and zeta potential were performed using SZ-100 device (Horiba, ABX SAS, Amadora, Portugal), and transmission electron microscopy (TEM) using JEOL 2100 200 kV operating at 200 kV (Izasa Scientific, Carnaxide, Portugal). TEM samples were prepared by placing and drying 5 μL of 20 mg L^{-1} NPs dispersion in ultrapure water on formvar/carbon-coated copper 200 mesh grids for citrate-P25 TiO_2 NPs and carbon-coated titanium 400 mesh grids for PVP-15 nm Ag NPs.

2.2. Diet formulation

Commercial pellets (Biomar Iberia, S.A.) were used as feeds for the turbots during the trials. NPs were incorporated in the pellets except for the control group. The pellets were coated with a premix that contributed to the even distribution of NPs in feeds. This premix was obtained by adding micronized calcium carbonate ($CaCO_3$, C.T.S. España S.L.) to the NPs, corresponding to 5% of the weight of pellets. Then, this premix was added to pellets until achieving 0.75 or 1.5 mg kg^{-1} of fish per day (for each NPs). Although these concentrations are higher than expected in the environment (or in aquaculture facilities), they were expected to allow us to understand the effects of NPs at the proteomic level during reasonable exposure periods.

2.3. Experimental design

Two independent experimental trials, each one with one of the two nanoparticles – citrate-P25 TiO_2 and PVP-15 nm Ag NPs, were carried out at the facilities of the Centro Tecnológico del Cluster de la Acuicultura (CETGA, Spain). In each trial, juvenile turbots (weight range between 45 and 50 g at TiO_2 NPs trial, and between 70 and 75 g at the Ag NPs trial) were kept in open flow systems composed of 1 m^3 indoor tanks (1 m × 1 m × 1 m, 50 fish per tank) with constantly running pre-filtered seawater (50 μm) and 35‰ salinity. Fish were allowed to acclimate for 1 week before each trial. The mean water temperature was 14.0 ± 1.2 °C and 15.5 ± 1.5 °C (natural environment temperature) for TiO_2 and Ag NPs trials, respectively, and photoperiod was set at 14h:10h (light:dark) along the experiments.

All fish groups were equally fed four times per day by hand (1–2% body weight of daily feeding rate) for 14 days. Three concentrations of each nanoparticle (TiO_2 or Ag) were tested: 0 (control group), 0.75 (*lower concentration*) and 1.5 (*higher concentration*) mg of NPs per kg of fish per day (three tanks per treatment group, see section 2.2 for further details on diet formulation). Observations of the fish health and behavior were performed daily.

Fish were weighed and killed on day 14 by overexposing to MS-222 (Sigma-Aldrich). Samples for analytical quantification, histology and proteomics were collected in accordance with the procedures described below in the corresponding sections. All experimental procedures were carried out in accordance with European Union and Spanish regulations (R.D. 53/2013 (BOE, 2013), and Council Directive 2010/63/EU (European Union, 2010)) for the protection of animals used for experimental purposes by personnel qualified in animal experimentation in authorized facilities by competent Spanish authority (REGA ES150730055401).

2.4. Analysis of NPs and total Ti and Ag in fish tissues

The determinations of total titanium and silver, and TiO_2 and Ag NPs in the liver, kidney and also muscle (inc. skin) of turbot were performed by ICP-MS/spICP-MS with a NexION 2000 ICP-MS (PerkinElmer, Waltham, MA, USA, detailed procedures are described in Supplementary Material 2, SM2). For each level of element equivalent dose, two specimens were taken, dissected and each organ treated (digested or the nanoparticles extracted) in duplicate. Enzymatic hydrolysis of the samples was used for TiO_2 NPs and Ag NPs extraction. Extracting solution consists of pancreatin and lipase (8 g L^{-1} each one (Ti) or 5 g L^{-1} each one (Ag), freshly prepared in 0.2 M NaH_2PO_4/0.2 M NaOH (pH 7.4) from *Candida rugose* (Sigma Aldrich, Osterode, Germany). Enzymatic hydrolysis was performed in duplicate per specimen by mixing approximately 1.0 g (*ww*) of homogenized samples and 7.5 mL of enzymes solution and stirring (orbital – horizontal shaking) at 180 rpm and 37 °C for 12 h. Before spICP-MS measurements for TiO_2 NPs and Ag NPs, glycerol at 1% (*v*/*v*) was used as a solvent for diluting enzymatic digests. Dilutions implied 1:100 to 1:500 factors depending on the sample to ensure an adequate TiO_2 NPs or Ag NPs concentration for spICP-MS assessment. After dilution, the mixtures were sonicated. Sample introduction flow rate and transport efficiency (TE%, measured by using the 49.6 nm Au NanoComposix material diluted at a concentration of 9.89 × 10^4 nanoparticles mL^{-1} in ultrapure water) were calculated before each measurement section. TE% was automatically calculated by using the SyngistixTM Nano Application software. Under the same instrumental conditions as those used for Ti/Ag, but monitoring *m*/*z* 197 for Au, the obtained TE% were within the 6–8% range. Finally, measurements were performed by using dissolved (ionic) titanium or silver aqueous standards from 0 to 10 (Ti)/0 to 5 (Ag) μg L^{-1}. SyngistixTM Nano Application software performs directly the calculation of TiO_2 NPs/Ag NPs concentration and size distribution. Microwave-assisted acid digestion of samples was used for measurements of total Ti and Ag, using Teflon vessels and covers. Each sample (approximately 1.0 g, *ww*) was mixed in duplicate with ultrapure water (4.0 mL), 69% (*w*/*v*) HNO_3 (3.0 mL), and 33% (*w*/*v*) H_2O_2 (1.0 mL) and subjecting the reactors to microwave irradiation. Acid digests were analysed for total Ti and Ag by ICP-MS under the operating conditions listed in SM2. Ionic titanium [$(NH_4)_2TiF_6$ 1000 mg L^{-1}] and ionic silver ($AgNO_3$ 1000 mg

L^{-1}) used for ICP-MS calibration, were purchased from Merck (Darmstadt, Germany). Gold nanoparticles solution used for transport efficiency determination was prepared from PEG-COOH gold nanospheres (49.6 nm, 9.89 × 10^6 particles mL^{-1}, Nanocomposix, San Diego, CA, USA).

2.5. Histology sample preparation and TEM

After 14 days of exposure two turbots from each treatment group were used to collect fragments of kidney, liver and also muscle (including skin). The fragments were fixated overnight at 4 °C in a mixture of 2% paraformaldehyde and 2.5% glutaraldehyde in 0.1 M sodium cacodylate buffer, followed by routine processing for TEM. Briefly, the fragments were post-fixated in a 1% osmium tetroxide solution, dehydrated with increasing ethanol (from 50 to 100%) and with a final emersion on propylene oxide. The infiltration was made in mixtures of propylene oxide: epoxy resin (EMBed-812 kit) at different proportions, increasing the amount of resin to finally have just epoxy resin. The cure of the blocks was at 60 °C, for three days.

Ultrathin sections (≈80 nm thick) were made in a PowerTome PC ultramicrotome (RMC Boeckeler, USA), with a diamond knife (Diatome) and placed on formvar/carbon 200 mesh grids for TiO_2 NPs and titanium 100 mesh grids in the case of Ag NPs. TEM micrographs of the sections were taken with a JEOL JEM 1010 transmission electron microscope operating at 100 kV. Size analysis of lipid droplets in liver' micrographs was performed in ImageJ. The software was calibrated by adding in the "scale calibration" the ratio pixel: nanometer of the image' magnification. Then, the major axis of the lipid droplet was used as the indicator for diameter for each condition (control, 0.75 and 1.5 mg kg^{-1}).

2.6. Proteomic analysis procedures

2.6.1. Protein extraction and sample preparation

Liver and kidney samples from fish of each treatment group (one sample from each tank, comprising tissues of 3 organisms from) were stored at −80 °C until further proteomic sample preparations. Following previously described protocols (Wiśniewski et al., 2009; Campos et al., 2015, 2016; Romeu et al., 2021), SDT buffer (0.5 g FW mL^{-1} SDT) and protease inhibitors (1:100, PIs, Roche, 11697498001, Basel, Switzerland) were added to both liver and kidney tissue samples. These samples were then sonicated (6 × 3 s and 23 kHz, 60 μm of amplitude) and incubated for 2 h at room temperature (RT). Then, the samples were heated for 3 min at 95 °C and centrifuged at 16,000 g for 20 min. The total protein concentration of the supernatant was estimated by optical density (OD) absorbance measurement at 280 nm using a DeNovix DS-11 Spectrophotometer (Protein A280 application, DeNovix Technologies, Wilmington, Delaware, USA). The extracted protein was stored at −20 °C until further processing.

The Single-pot, solid-phase-enhanced sample preparation procedure (SP3) (Hughes et al., 2019) with the adaptions of Araújo et al. (2021) was used. Prior to digestion, 100 μg of proteins (approx. 5 μL of the extract) were reduced in 45 μL SDT buffer. Then, alkylation of samples was performed with 10 μL of 0.1 M iodoacetamide (AppliChem) in 8 M Urea, 0.1 M Tris/HCl pH 8.5 for 30 min in the dark (RT).

Magnetic beads (Sera Mag SP3 beads, CAT#45152105050250 and CAT#65152105050250, GE Healthcare) were initially washed and reconstituted in deionized water (HPLC grade, VWR) at a final concentration of 10 μg $μL^{-1}$ (from an initial stock concentration of 50 mg mL^{-1}), using a magnetic rack (MagnaRack, Invitrogen) for 1 min. A 10:1 *v/v* ratio (beads:proteins) was reached by adding 100 μL of beads suspension to each tube and followed by 160 μL of absolute ethanol (molecular biology grade, Fisher). Incubation was performed in a Thermomixer (shaking for 10 min at RT). Sample tubes were then placed in the magnetic rack and supernatant was removed. Beads were gently reconstituted in 180 μL of 80% ethanol, and a cleaning step with the tubes being placed at the magnetic rack and discarding the supernatant was performed three times. The extraction of the beads with the peptides was performed by adding 100 μL of ammonium bicarbonate (0.1 M pH 8) containing 0.04 μg/μL Trypsin/rLys-C Mix (MS grade, Promega) to each tube at a 1:50 ratio (enzyme:protein). An incubation period of 14 h at 37 °C with mixing (0.1g) was followed and then, 1.3 mL of 100% acetonitrile (HPLC grade, Chem-Lab NV) was added and incubated for 18 min. Beads were then spun down and tubes placed in the magnetic rack. The supernatant was discarded, and the beads were washed twice with 180 μL of 100% acetonitrile. After removal of the supernatant, 100 μL of 0.05 M ammonium bicarbonate (Fluka) was added to the tubes and incubated for 5 min at 1000 rpm. After the beads removal, the supernatant containing the tryptic peptides was transferred to new 1.5 mL tubes. The peptide concentration was estimated at A280 and acidification was performed by adding 20 μL of 5% *v/v* formic acid (Optima LC/MS grade, Fisher Chemical) to the samples. Afterwards, tryptic peptides were dried in a Concentrator Plus vacuum rotator (Eppendorf, Hamburg, Germany) and resuspended in 25 μL of 0.1% *v/v* formic acid in deionized water. The final concentration of peptides was estimated at A280 nm. In total, 36 peptide samples were prepared for MS/MS analysis, belonging to kidney and liver samples of tested fish (control, *lower* and *higher* TiO_2 and Ag NPs concentration groups).

2.6.2. LC-MS/MS analysis

The LC-MS/MS analysis was performed using a nano-LC coupled to Q Exactive HF Hybrid Quadrupole-Orbitrap Mass Spectrometer (Thermo Scientific, Waltham, MA, USA). The peptides were separated by reverse phase chromatography with an EASY nLC 1200 system (Thermo Scientific). After the injection of peptides into a pre-column (Acclaim PepMap 100, 75μm × 2 cm, Thermo Scientific), their separation was performed using an EASY-Spray C18 reversed-phase nano LC column (PepMap RSLC C18, 2 μm, 100A 75 μm × 25 cm, Thermo Scientific) by a gradient of 0.1% formic acid in water (A) and 0.1% formic acid in 80% acetonitrile (B) as follows: from 6% B to 40% B in 80 min; from 40% B to 100% B in 20 min at a flow rate of 0.3 μL min^{-1}. Separated peptides were electrosprayed and analysed using a Q Exactive HF mass spectrometer (Thermo) operated in positive polarity in a data-dependent acquisition mode. Full scans were performed at 120 000 resolution at a range of 380–1400 *m/z* and the top 15 most intense multiple charged ions were isolated (1.2 *m/z* isolation window) and fragmented at a resolution of 30 000 with a dynamic exclusion of 30.0 s. All samples were analysed in triplicates.

2.6.3. Protein identification

The generated raw files were analysed using Sequest HT in Proteome Discoverer (v. 2.4.0.305, Thermo Scientific). All searches were performed using *Scophthalmus maximus* protein database (49819 entries, downloaded from National Center for Biotechnology Information database on 19/01/2021). The search parameters were: trypsin as the digestion enzyme with maximum number of 2 missed cleavages, fragment ion mass tolerance of 0.02 Da, parent ion tolerance of 10 ppm; carbamidomethylation of cysteine used as fixed modification and oxidation of methionine was specified as variable modification. Scaffold (v. 4.11.1, Proteome Software Inc., Portland, OR) was used to validate protein identifications. Proteins were accepted if their identification probability was greater than 99.9% (using the Scaffold local FDR algorithm), and protein identification was based on a minimum 2 peptides with at least 95.0% peptide identification, assigned by the Protein Prophet algorithm (Nesvizhskii et al., 2003). Proteins that contained similar peptides and could not be differentiated based on MS/MS analysis alone were grouped to satisfy the principles of parsimony. Proteins sharing significant peptide evidence were grouped into clusters and used for analysis.

2.6.4. Differentially expressed proteins

Protein expression analysis was performed using normalized average

precursor ion intensity (API). API values were squared root transformed and statistical differences between experimental groups were analysed in R software (R Core Team, 2021). Only those proteins that were identified in at least 2 of the 3 replicates were filtered for further analysis. Data were normalized with the *normalize_vsn* function and missing values were imputed using *impute* function from *DEP* package (Differential Enrichment analysis of Proteomics data, Zhang et al., 2018). For this imputation was selected a probabilistic minimum with the "MinProb" method, which uses a random draw from a Gaussian distribution centred around a minimum fixed value. With these data of protein expression, differences between treatments were tested with multiple comparisons based on Bayes sphericity test, implemented in the *test_diff* function from *DEP* package (Zhang et al., 2018). Differentially expressed proteins (DEPs) were selected with the criterion of an alpha of 0.05 together with a log fold change greater than 1.

2.6.5. Functional annotation

DEP sequences were matched to zebrafish (genome assembly GRCz11, NCBI) by running the local BLASTp function from Blast2Go program version 5 (basic), setting a cut-off e-value of $1e^{-3}$. This analysis was necessary given the poor functional annotation of turbot genes and proteins. Functional analysis was then carried out based on the information from the homologous proteins from zebrafish. The STRING: functional protein association networks (https://string-db.org/) was used for searching protein interaction evidence studying the interactions between proteins and the potential molecular pathways affected by NPs using zebrafish information. Sources of protein interaction evidence included: text mining, experiments, databases, co-expression, neighbourhood, gene fusion and co-occurrence. The results of Kyoto Encyclopedia of Genes and Genomes (KEGG), in STRING, were used following a full network with medium confidence of 0.400 and FDR stringency of 5%. A minimum number of nodes was added if needed to reach a significant PPI enrichment p-value. Proteins were then grouped into clusters in STRING using the k-means clustering method.

2.7. Statistical analysis

The total element concentrations (Ti or Ag) at 14 days were compared against time 0 with pairwise t-tests. Comparisons among tissues for the same days/ages were also performed with pairwise t-tests. Pairwise *t*-test were also used for comparing hepatocyte lipid droplets sizes and density. One-Way ANOVA (followed by Dunnetts' test when adequate) was used to study the existence of significant differences in fish weight after 14 days, between control group and NPs exposed fish, after normality and homoscedasticity (Brown-Forsythe) were tested. SigmaPlot v.12 Systat Software Inc was used for the statistical analysis. A level of significancy of 0.05 was considered. Results are expressed as mean ± standard error (SE) if not mentioned otherwise.

3. Results

3.1. Characterization and behavior of nanoparticles

TEM analysis reveals that citrate-P25 TiO_2 NPs have a high tendency to form aggregates involving spherical TiO_2 NPs with a primary size of 29.0 ± 0.4 nm (Supplementary Material 1, SM1).

In the case of PVP-15 nm Ag NPs, TEM image in SM1 shows that these NPs are well-dispersed with a primary size of 24.0 ± 0.5 nm. This primary size is bigger than the statement for the supplier (SSNAno), which could be attributed to the high dispersion and reactivity of silver provoking higher variation batch-to-batch (Dawadi et al., 2021).

The hydrodynamic diameter registered was 166 ± 1 nm and 7589 ± 1025 nm for citrate-P25 TiO_2 NPs and 49 ± 01 nm and 47 ± 1 nm for PVP-15 nm Ag NPs in ultrapure and artificial seawater, respectively (see SM1). Clearly, citrate-P25 TiO_2 NPs formed small aggregates in ultrapure water, which is in agreement with TEM analysis, while they aggregated completely in artificial seawater. The zeta potential measurement showed that the surface charge of TiO_2 NPs in seawater was almost null (−3 mV), while they presented a negative surface charge in ultrapure water (−81 mV). This explains the massive aggregation that occurred in artificial seawater. The compression of the electric double layer (EDL) promoted the high ionic strength of seawater and induced the aggregation in citrate-P25 TiO_2 NPs because citrate only offers electrostatic stability (Moore et al., 2015). In the case of PVP-15 nm Ag NPs, the NPs remained colloidally stable in both media even when the surface charge decreased in artificial seawater (−24 mV in ultrapure water VS -9 mV in artificial seawater) because PVP coating provides a stabilization by electrosteric repulsion, as reported previously (Quarato et al., 2021).

3.2. Fish mortality and growth

Along the 14-day exposure and at the end of the trials with TiO_2 and Ag NPs, the fish mortality in the control groups and in the treatment groups of exposed organisms was null. Besides, noticeable physiological alterations (e.g.: external lesions) were not observed at the end of the two trials. After 14 days, 16.1% lower fish weight was observed after exposure to the *Higher* concentration of TiO_2 NPs, when compared to control (55.8 ± 3.46 g and 66.6 ± 5.47 g, respectively, $p < 0.05$, Supplementary Material 3, SM3), which was possibly related to an apparent reduction of feed intake. At the end of the Ag NPs trial, no significant differences in fish weight were detected between NPs treatments and control group ($p > 0.05$, SM3).

3.3. Chemical analysis of tissues

At the TiO_2 NPs trial, the NPs were not detected in any of the tissues tested (liver, kidney and muscle, Limit of Detection 2.52×10^4 part g^{-1}) neither at day 0 nor at the end of the test (14 days) in fish groups exposed to *Low* and *High concentrations*. Total titanium was detected on liver and muscle of turbot, including at day 0, while the levels in kidney were lower than the Limit of Quantification (0.005 μg g^{-1}) in all samples (Table 1). Liver showed higher titanium concentrations than muscle at the beginning of the test. In liver, the titanium levels were significantly higher on *Low concentration* group when compared to day 0. Similarly, at the Ag NPs trial, the NPs were not detected on the tissues (liver, kidney and muscle, Limit of Detection 7.51×10^4 part g^{-1}) at day 0 and at the end of the test (14 days) at the fish groups exposed to *Low* and *High concentrations*. Total silver, on the other hand, was detected in liver and

Table 1
Quantification of total titanium and silver in liver, kidney and muscle of turbot. * represents statistical differences between each NPs doses with day 0, within each tissue (pairwise *t*-test, $p < 0.05$), [a] represents statistical differences between liver, kidney or muscle (within each trial) for the same NPs doses (pairwise *t*-test, $p < 0.05$).

Exposure (days)	Equivalent dose (mg/Kg)	Liver (μg g^{-1})	Kidney (μg g^{-1})	Muscle (inc. skin, μg g^{-1})
Citrate-TiO_2 NPs trial Total Titanium				
0	0	0.079 ± 0.018	<LOQ	0.015 ± 0.004
14	0.75 (*Low*)	0.910 ± 0.063*[a]	<LOQ	0.033 ± 0.021
14	1.5 (*High*)	0.317 ± 0.175	<LOQ	0.016 ± 0.001
PVP-Ag NPs trial Total Silver				
0	0	0.008 ± 0.008	<LOQ	<LOQ
14	0.75 (*Low*)	0.328 ± 0.168	0.012 ± 0.005	<LOQ
14	1.5 (*High*)	0.302 ± 0.020*[a]	0.009 ± 0.004	<LOQ

LOQ: 0.005 μg g^{-1}

kidney of fish exposed to the Ag NPs while in the muscle the silver levels were below the Limit of Quantification (0.005 μg g^{-1}, Table 1). The highest values were found in liver when compared to kidney.

3.4. Histology

The TEM analysis did not detect TiO_2 or Ag NPs in liver or kidney of turbot. Furthermore, evidence of alterations in the ultrastructure of the tissues or cells was not detected (Figs. 1 and 2). However, in liver, differences in hepatocytes' lipid droplets (LDs) properties were observed. Hepatocytes' in turbot exposed to *Higher concentration* of TiO_2 NPs showed significantly bigger LDs (2.64 ± 0.08 μm) than controls (1.94 ± 0.07 μm) and a higher diameter range (Fig. 1, Supplementary Material 4: SM4.1 and SM4.2). The density of LDs was also significantly lower in fish exposed to *Lower concentration* of TiO_2 NPs. In the case of turbot exposed to *Lower concentration* or *Higher concentration* of Ag NPs, hepatocytes' LDs were significantly smaller in terms of mean size (2.8 ± 0.1 μm and 2.8 ± 0.1 μm when compared to control (3.2 ± 0.10 μm) and clear trends regarding the diameter range and density of LDs were inexistent (Fig. 2, Supplementary Material 4: SM4.1 and SM4.3).

3.5. Proteome alterations

3.5.1. Protein identification

The total number of proteins identified in the experimental trial with feeds that contained TiO_2 NPs were 1415 and 1651 in liver and kidney, respectively (Fig. 3), after following a proteome shotgun analysis. At the Ag NPs trial, 1572 and 2736 proteins were identified in liver and kidney, respectively (Fig. 3, the complete list of proteins identified, and respective abundances are reported in Supplementary Material 5: SM5.1-4). Overall, for both trials, more proteins were identified in kidney than in liver. Moreover, the overall percentage of identified proteins shared among the three experimental groups was also similar in both tissues and trials (between 58.5% and 67.7%, Fig. 3).

In the case of TiO_2 NPs trial, 247 liver proteins were identified in only one of the experimental groups (exclusive proteins, most of them in control group). In this trial, 1326 kidney proteins (80% of the total) were identified in more than one experimental group (shared proteins), and 325 were exclusive proteins (most of them in NPs exposed groups).

In the case of Ag NPs trial, among the 1572 proteins identified from the liver samples, 1200 proteins (76% of the total) were present in more than one experimental group (shared proteins) and 372 were exclusive proteins (most in *Lower concentration* group). Furthermore, the proteins

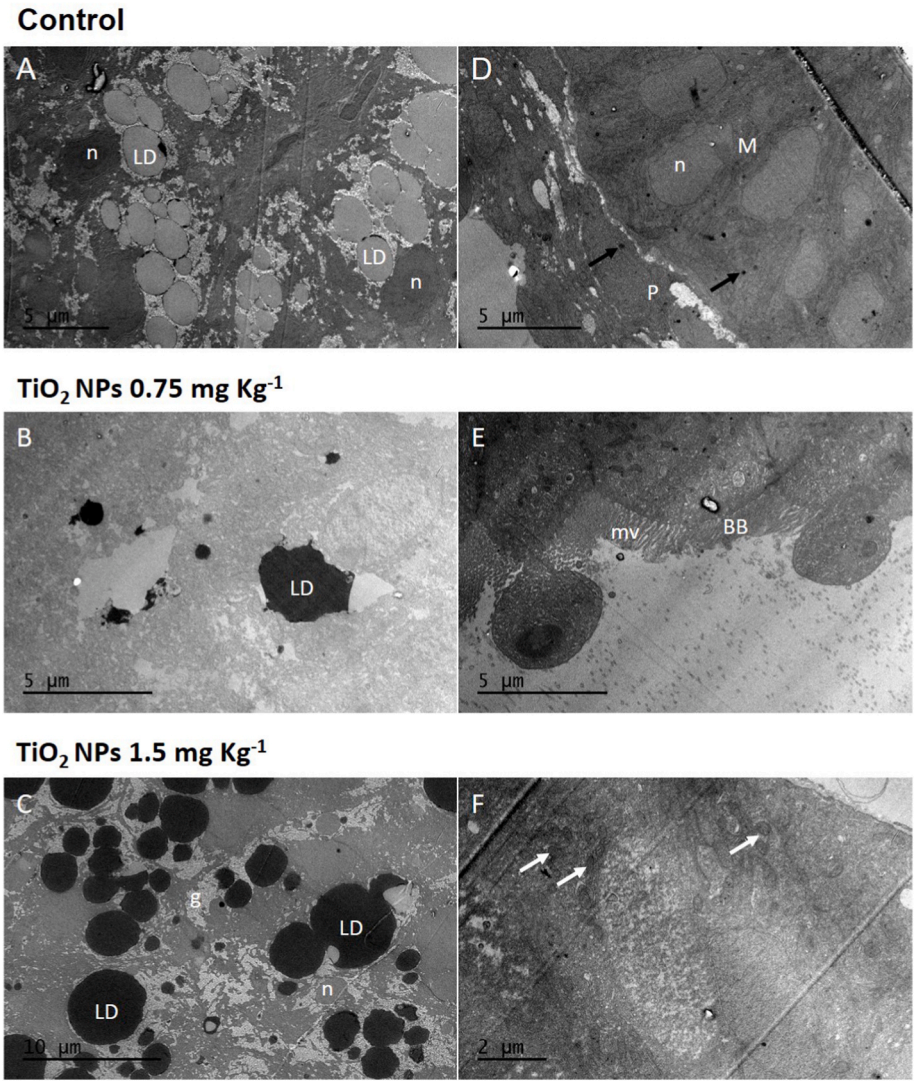

Fig. 1. Transmission electron micrographs of control cells from liver hepatocytes (A) and kidney glomerulus (D) and after dietary exposure to citrate-P25 TiO_2 NPs (B and C; E and F, respectively). LD = lipid droplets, n = *nucleus*, mv = *microvilli*, g = glycogen, BB = brush border of proximal tubule, P = podocyte, M = mesangial cells, white arrows point to mitochondria, black arrows point to electron dense accumulates (no NPs).

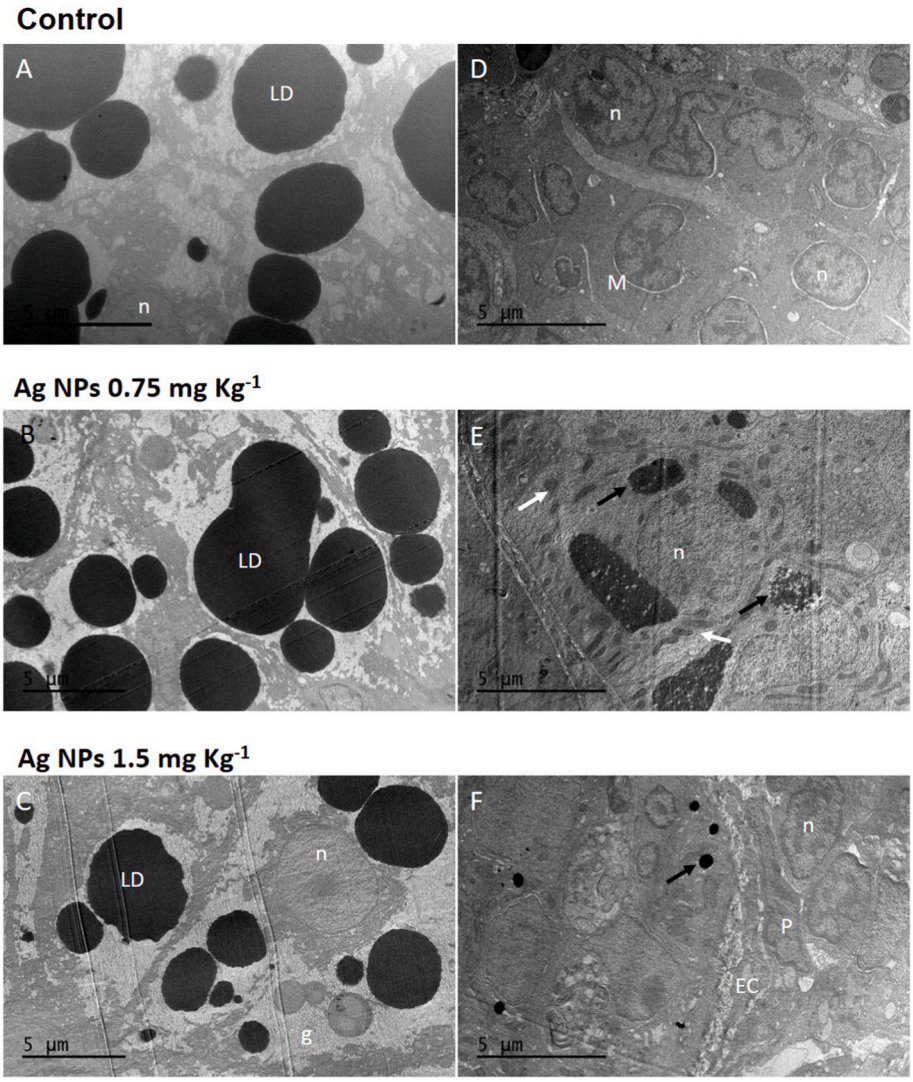

Fig. 2. Transmission electron micrographs of control cells from liver (A) and kidney glomerulus (D) and after exposure to PVP-15 nm Ag NPs (B and C; E and F, respectively). LD = lipid droplets, n = *nucleus*, mv = *microvilli*, g = glycogen, P = podocyte, M = mesangial cells, EC = endothelial cells, white arrows point to mitochondria, black arrows point to electron dense accumulates (no NPs).

identified in the kidney in more than one experimental group were 2269 (83% of the total identified in this tissue), and 467 were exclusive proteins.

3.5.2. *Differential protein expression and functional analysis*

Differences in protein expression were investigated in the R program, using the *DEP* package (Zhang et al., 2018) and overall differences between experimental groups and proteins can be inferred from cluster analysis displayed in Fig. 4. Information supporting Fig. 4, namely concerning protein name, accession number, expression and statistics of DEPs, is reported in Supplementary Material 5: SM5.5-8.

The statistical analysis showed higher numbers of DEPs in Ag NPs trial than in TiO_2 NPs trial (113 and 39 exclusive proteins, respectively). In addition, a greater number of DEPs was observed in kidney than in liver in both trials, which is in agreement with the overall number of identified proteins.

The TiO_2 NPs trial revealed 15 DEPs, in comparison to control, in turbot liver, six of which were in *Lower concentration* group and nine DEPs in the *Higher concentration* group (Fig. 4, Supplementary Materials 5: SM5.5-8). In turbot kidney, a total of 12 DEPs were identified in the *Higher concentration* group and no protein expression changes were found in *Lower concentration* group. when compared to control. Among the total number of DEPs identified in TiO_2 NPs, a similar number of proteins was up-regulated and down-regulated in liver (between three and five DEPs for each *lower* or *higher* compared to control, respectively). In the case of the kidney, a higher number of DEPs were up-regulated (nine proteins) in comparison to the down-regulated DEPs (three proteins) in the *higher* concentration group (Fig. 4).

In the case of Ag NPs trial, 39 DEPs were found, when compared to control, in the liver, 19 of which were in *lower* group and 20 in *higher* concentration group. In kidney, 73 DEPs were observed, 38 of which were in *lower* concentration group and 35 in *higher* concentration group. In liver, the number of up-regulated proteins was 11 and 18 in the *lower* and *higher* concentration groups respectively; while in kidney the up-regulated proteins were 34 and 30, respectively. In total, 13 and 19 proteins displayed expression differences between groups (*lower* vs *higher* concentration groups) exposed to TiO_2 NPs and Ag NPs, respectively, with most of these differences being observed in kidney (Fig. 4).

3.5.3. *Protein functional analysis*

3.5.3.1. TiO_2 NPs. Functional analysis with STRING web tool revealed that the proteins altered by TiO_2 NPs in liver of turbot (*lower concentration*) could be related with metabolic pathways, purine metabolism,

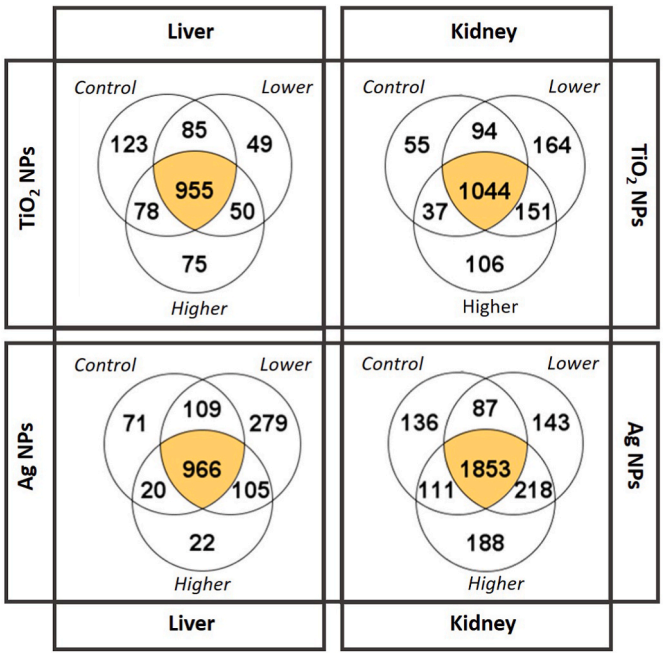

Fig. 3. Venn diagram representing shared and unique proteins identified in turbot tissues from experimental trials with citrate-P25 TiO_2 and PVP-15nm Ag NPs. *Lower* and *Higher concentrations* refer to 0.75 and 1.5 mg of NPs per kg of fish per day, respectively.

drug metabolism and pyrimidine metabolism (Fig. 5, Supplementary Material 5: SM5.9 and SM5.10). Among the identified proteins, two of them are strongly associated with these processes: the protein UMP-CMP kinase (*cmpk*) that catalyses the phosphorylation of pyrimidine nucleoside monophosphates at the expense of ATP and plays an important role in *de novo* pyrimidine nucleotide biosynthesis, and the protein carbonic anhydrase (*cahz*). When analysing the exposure to the *higher* TiO_2 NPs concentration, STRING analysis suggests that alterations in liver proteins could involve ribosome, peroxisome and gene transcription functions. Among these proteins are Aminopeptidase-like 1 (*npepl1*), the Sterol carrier protein 2b (*scp2b*), and the HECT, UBA and WWE domain containing 1 (*huwe1*) respectively. Other roles suggested for these proteins are the regulation of intracellular cholesterol transport (*scp2b*), amino acid cleavage (*npepl1*) and protein ubiquitination (HECT), sumoylation (UBA, *huwe1*).

In the kidney, the exposure to the highest concentration of TiO_2 NPs, affected several proteins involved in metabolic pathways. Phosphoinositide phospholipase C (*plcd1b*) is known to be involved in lipid catabolic processes whereas profilin (*pfn2*) and transgelin (*tagln*) but also adducin 3 gamma (*adde3a*) are involved in cytoskeleton organization (bind to actin filaments). Moreover, Copine III (*cpne3*) is suggested to have a role in ERBB2 signalling pathway and other proteins, chloride intracellular channel protein (*clic1*), solute carrier family 22 member 2 (*SLC22A2*) and glutamate receptor (*grin3ba/loc566411*), are known to mediate the transport of a variety of ionic compounds including chemical messengers (neurotransmitters) amino acids, toxins, xenobiotic substances, and to participate in cellular signalling mechanisms.

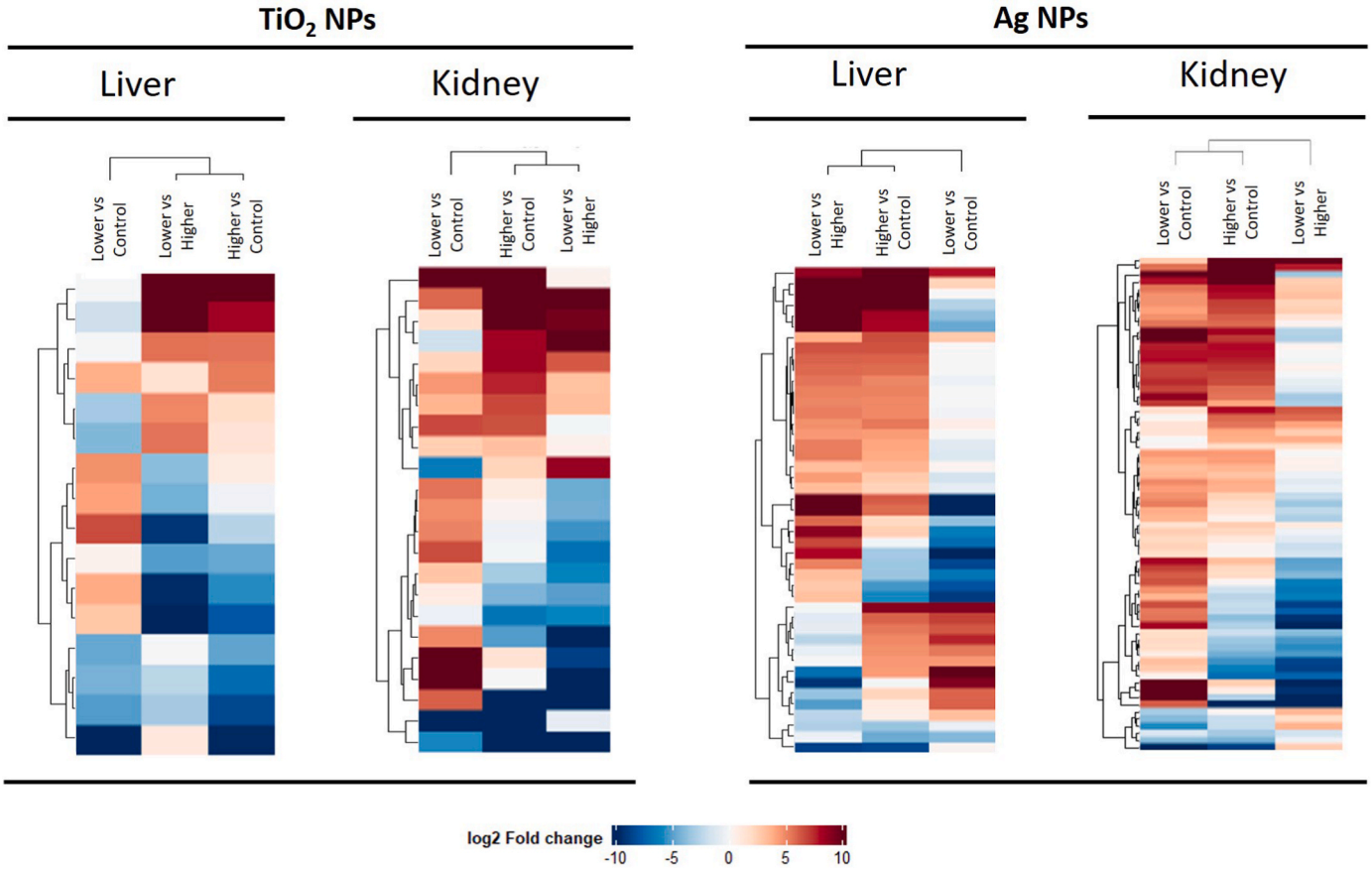

Fig. 4. Graphical representation (heatmap) of protein expression alterations (contrast, k-means) in TiO_2 and Ag NPs trials. *Lower* and *Higher concentrations* refer to 0.75 and 1.5 mg of NPs per kg of fish per day, respectively. Colour scale represents protein fold changes observed between experimental groups. The rows represent DEPs clustered by k-means and columns the comparisons made between experimental groups (protein names and detailed information of statistics are reported in Supplementary Material 5.5-8). (For interpretation of the references to colour in this figure legend, the reader is referred to the Web version of this article.)

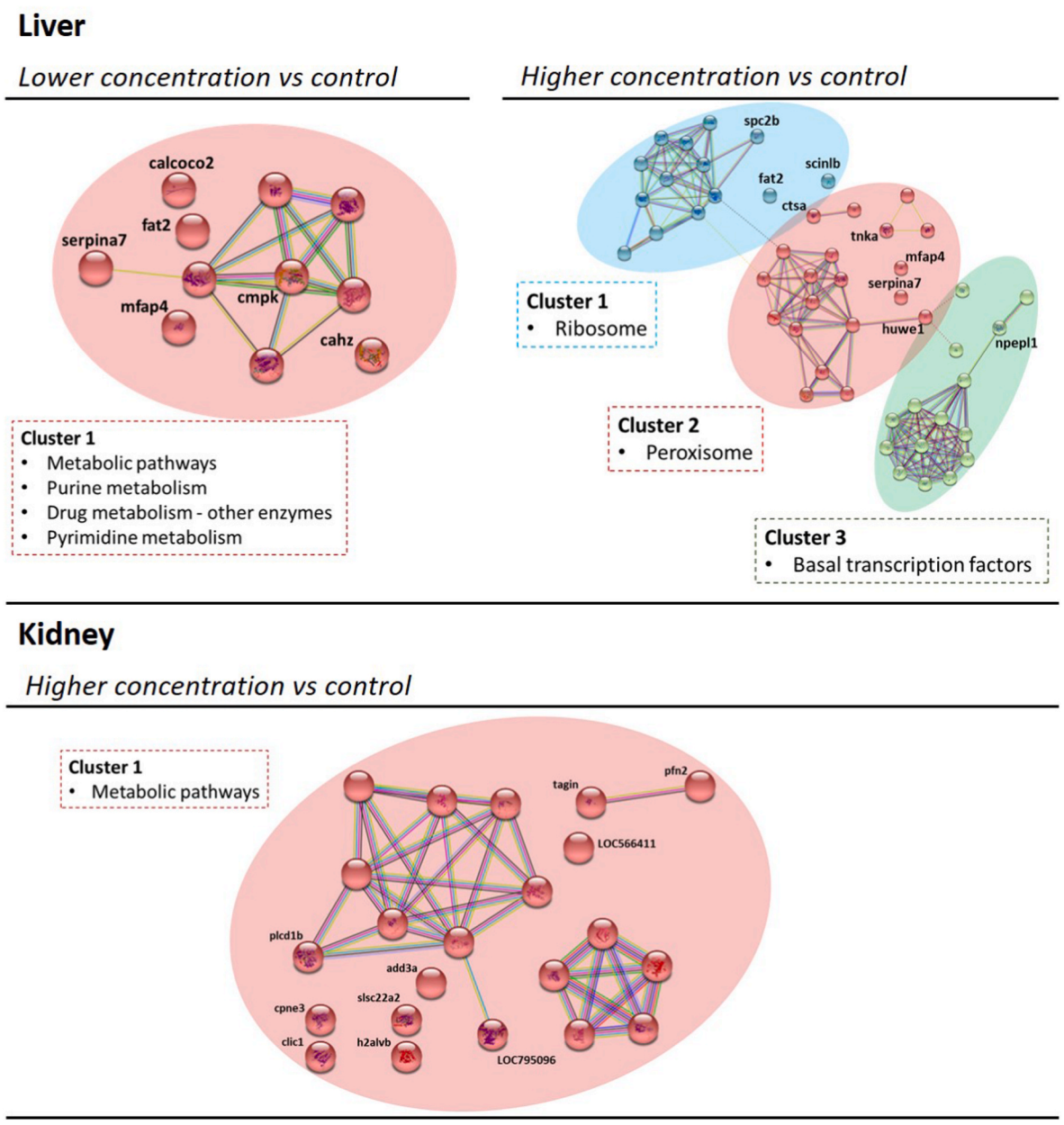

Fig. 5. Predicted functional associations of turbot liver and kidney proteins exposed to TiO_2 NPs. *Lower* and *Higher concentrations* refer to 0.75 and 1.5 mg of NPs per kg of fish per day, respectively. The DEPs (zebrafish homologous) have their identification in the network whereas other proteins displayed are potential significant interactors predicted by STRING database (https://string-db.org/). Protein identity is displayed using gene identifier codes. The terms in the legend of each network refer to the KEGG terms. Statistical parameters of each term are presented in Supplementary Material 5: SM5.11.

3.5.3.2. Ag NPs. The STRING analysis showed that proteins affected by Ag NPs exposure are associated with generic biological processes and ribosome functions (Fig. 6, Supplementary Material 5: SM5.9 and SM5.10). Proteins affected in liver were also linked with spliceosome functions (*sf3b1*) and several energy-related processes, namely butanoate metabolism, synthesis and degradation of ketone bodies and amino sugar and nucleotide sugar metabolism (e.g.: *bdh1*, *pgm3*). Other possible roles can be attributed to proteins affected in liver linked to cell signalling (*mif*, *gnb2l1*, *sec1418*, *calcoco2*), vesicle-mediated transport and intra-cellular trafficking (*snx5*, *ap1b1*, *sec23ip*, *ncl1*), synaptic transmission (*cel.1*), heme metabolism (*hpx*, *blvrb*), protein ubiquitination (*cand1*, *ddrgk1*), stabilization and degradation (*bhmt*, *cpb1*, *NHL repeat containing 3*), RNA binding and protein translation (*serbp1a*, *vars1*), ATP synthesis (*ndufs1*).

In the kidney, besides the functions associated with spliceosome, ribosome and oxidative phosphorylation, revealed with STRING analysis, other functions can be attributed to the proteins affected by Ag NPs in this organ. Among the proteins identified are several kinases (*csk*, *gnb2l1*, *pkn1a*), several proteins involved in protein folding mechanisms (*fkbp2*, *ppifb*, *pdia5*) and proteins involved in the ubiquitin-dependent protein degradation pathway (*skp1*, *rnf213a*, *usp10*). We also observe that a considerable number of proteins are related with membrane functions including endocytosis (*fnbp1b*, *flot1b*), intracellular protein transport (*scamp2*, *chmp4c*, *stx12l*), transmembrane transport (*slc25a21*, *tcirg1b*), mitochondrial fission (*mtfp1*) and protein insertion into mitochondrial inner membrane (*timm13*). Other proteins can be related with microtubule functions and cytoskeleton structure (*pafah1b1a*, *sept9b*).

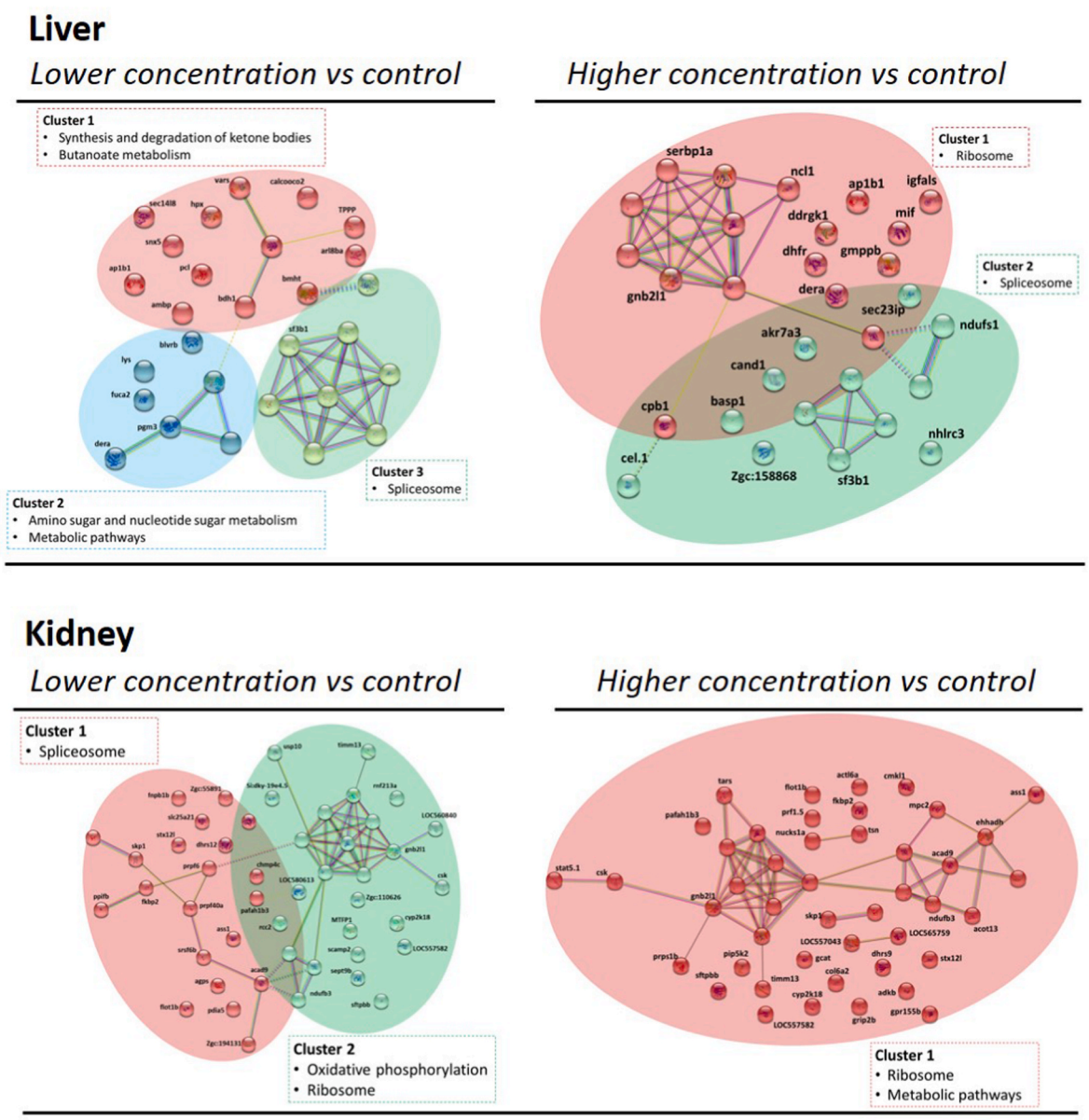

Fig. 6. Predicted functional associations of turbot liver and kidney proteins exposed to Ag NPs. *Lower* and *Higher concentrations* refer to 0.75 and 1.5 mg NPs per kg of fish per day, respectively. The DEPs (zebrafish homologous) have their identification in the network whereas other proteins displayed are potential significant interactors predicted by STRING database (https://string-db.org/). The terms in the legend of each network refer to the KEGG terms. Statistical parameters of each term are presented in Supplementary Material 5: SM5.11.

4. Discussion

There is a global concern about the increasing amounts of engineered inorganic NPs reaching aquatic environment. Therefore, in this work, alterations in tissues (liver and kidney) of a marine flatfish species, were studied in response to citrate-P25 TiO_2 and PVP-15 nm Ag NPs 14-day exposure through feeding, with particular attention to the alterations induced at proteomic level.

4.1. Accumulation of NPs in tissues

In the present work, although TiO_2 and Ag NPs were not detected in liver and kidney (or muscle) after the 14-day exposure, the titanium and silver elements were detected in higher amounts than at the beginning of the study. These facts suggest the transformation of NPs (i.e., aggregation, dissolution, sulfidation, etc.) inside the tissues of the organisms. The alteration of NPs properties can be expected following their lack of stability in certain conditions (e.g.: NPs-biomolecule interactions and media conditions on the organisms, Auría-Soro et al., 2019); however, it remains unclear how the mechanisms of aggregation occur. Another possible transformation of NPs that could occur is the dissolution of them after their uptake (Abbas et al., 2020). In fact, several reports have shown that Ag NPs can undergo either dissolution or sulfidation, or both transformation when they are uptaken by cells/organisms (Moore et al., 2015; Yue et al., 2017; Grasso et al., 2021; Khan et al., 2019). Distinct accumulation patterns to NPs exposure are expected in each organ, which can be associated with the contributions of different organs to the detoxification, excretion or uptake of exogenous substances (Bartucci et al., 2020). Kidney and liver have active roles in excretion or accumulation of NPs and thus, diverse and differential responses to exogenous compounds have been observed (Handy et al., 2008; Carvalhais et al., 2021). In the present work, the action of liver dealing with NPs is particularly relevant since the concentrations of titanium and silver were higher in this organ when compared to kidney (and muscle).

4.2. Alterations in hepatocytes

Despite the lack of evidences of NPs accumulation (by ICP-MS and TEM), it becomes clear from this study that exposure to citrate-P25 TiO_2 and PVP-15 nm Ag NPs induces biological responses, such as alterations in the size and density of LDs in hepatocytes. Lipid droplets in hepatocytes are often quite large (>1–2 μm diameter) and form by coalescence or through protein-mediated facilitated diffusion of neutral lipids (Gluchowski et al., 2017). Thus, the observation of bigger but fewer LDs with TiO_2 NPs exposure points to a process of LDs coalescence as the main cause of this difference. Coalescence is usual when there is insufficient phosphatidylcholine to cover the LDs surface to lower surface tension to maintain a metastable state (Gluchowski et al., 2017). However, it cannot be ruled out that the increase in the size of the LDs observed could be due to oxidative stress, as this kind of damage also leads to the accumulation of fatty acids within hepatocytes (Cichoż-Lach and Michalak, 2014). In the case of Ag NPs, the inexistence of effects on the number of LDs suggests a higher metabolization of the neutral lipids in turbot exposed to Ag NPs by lipolysis or liphophagy (Schott et al., 2019). Further discussion on these alterations is presented below.

4.3. Proteome alterations

In the present work, the protein profile of turbot kidney tissues comprised a higher number of identified proteins than liver tissues, resulting in a higher identification of DEPs in response to NPs exposure. In fish and also murine, kidney was reported to be severely affected by NPs, and effects related to the immune response (the main function of anterior kidney) or excretory system (the main function of trunk kidney) can be expected (Soulliere and Dixon, 2017; Bartucci et al., 2020; Takvam et al., 2021).

4.3.1. Titanium dioxide NPs

The number of metabolic processes potentially altered was higher in liver in comparison to the kidney. Previous works point out that TiO_2 NPs exposure can induce proteome alterations, genotoxicity, oxidative stress and cell apoptosis in rats, and that liver is one of the main organs affected by these NPs (Meena and Paulraj, 2012; Shakeel et al., 2016, Dhupal et al., 2018; Wani and Shadab, 2020, Cao et al., 2020). A series of effects of these NPs, including human liver steatosis, oedema and fibrosis was reported (Brand et al., 2020). The exposure to a wide range of exogenous stressors has been previously associated with alterations of several intracellular biochemical processes, resulting in the abnormal production of ATP and release of heat and chemical by-products (lactate and CO_2) into the extracellular environment (Picard et al., 2018; Briffa et al., 2020). The exposure to TiO_2 NPs was also previously associated with an extraordinary energetic expenditure, increased oxidative stress and mitochondrial damage and effects in lipid metabolism, which can result in an overall significant decrease in body weight (e.g.: Wang et al., 2010; Song et al., 2016; Carmo et al., 2019; Baranowska-Wójcik et al., 2020; among others). In the case of human bronchial epithelial cell lines, TiO_2 25 nm NPs exposure was previously associated with alterations of proteins with roles in glycolysis and citrate cycle (Ge et al., 2011). The alterations in metabolic processes that are suggested by the DEPs in TiO_2 NPs trial, could partially explain the previously described effects). In liver, these NPs could have affected purine metabolism, drug metabolism, pyrimidine metabolism, but also ribosome and peroxisome functions and gene transcription. Changes in proteins involved in the pathway of protein modification/degradation via ubiquitin were also denoted.

In kidney, proteomics results suggest alterations in lipid metabolism, cytoskeleton proteins and several cell membrane functions including transport of metabolites and signal transduction. Several of these pathways could be critical for kidney functions. Moreover, alterations in cytoskeleton could affect cell integrity. Therefore, the medium/long-term exposure effects to environmentally relevant concentrations and their possible effects on metabolic, energetic or lipid processes, and smaller growth deserves further studies.

The analysis of the results in the present study and the ones from Carvalhais et al. (2021), highlight that the route and the duration of the exposure are relevant parameters for TiO_2 NPs molecular effects. Those authors observed effects (including altered metabolic function after 7 days of exposure to slightly higher doses) on liver of younger juvenile turbots (20 g) intraperitoneally injected with P25 TiO_2 NPs, while kidneys were unaffected. In the present study, the alterations observed in the kidney at the protein level after 14-day feeding exposure, suggest impacts of the TiO_2 NPs on basal function of this organ in several ways, denoting its role in processes related to the uptake of contaminants through feeding. In this organ, we point out the adverse effects of the alterations in the cytoskeleton proteins and cell membrane functions. Such effects may be associated with later consequences in organisms' life cycle. However, further studies should be performed to support this hypothesis and confirm if this can also suggest that organisms can successfully deal with such exposure.

The action of NPs with specific coatings is important since effects vary depending on their surface and physicochemical properties (Shi et al., 2013; Auclair et al., 2019; Khan et al., 2019). Sodium citrate is one of the most common molecules used for coating metal NPs, including TiO_2 NPs. It is a good chelating agent (particularly for metals) and prevents agglomeration, one of the main challenges for NPs functionalization (Kim et al., 2014). This non-toxic antioxidant and anticoagulant is also present in almost all organisms, with several biological functions, including cellular respiration and metabolism, with a relevant role in the Krebs cycle, and oxidation resulting in energy production (Williams and O'Neill, 2018; Martínez-Reyes and Chandel, 2020). TiO_2 NPs have been pointed to increase energy expenditure, and citric acid and its salts should have a positive contribution to better growth of fish (Lückstädt, 2008; Shah et al., 2015; Zhang et al., 2016a; Sotoudeh et al., 2020). Therefore, the use of citrate to the tested organisms could in theory add extra energy availability, inducing weight gain. However, that situation was not observed, suggesting that the putative benefits of the presence of citrate were apparently masked by the toxic effects of TiO_2 NPs.

As in our work, Tucci et al. (2013) also observed effects in nucleotide synthesis in response to TiO_2 NPs exposure. Since *de novo* purine biosynthetic pathway is an energy-intensive pathway (Pedley and Benkovic, 2017), which seems to be affected by TiO_2 NPs exposure, energetic unbalances of turbot may result from the exposure to this NP.

The combined effects of TiO_2 NPs and other stressors or conditions are also of concern, since decreased immune system (namely, decreased resistance against bacterial pathogens) (Jovanović et al., 2015) and altered antioxidant systems in the presence of other metals have been previously described in fish (Vicari et al., 2018).

Finally, particular attention should be given to specific altered proteins in response to TiO_2 NPs exposure. For instance, *cmpk1* is an enzyme required for nucleic acid biosynthesis. The functional analysis revealed that pyrimidine metabolism was altered in both tissues and this function is related to *cmpk1* action. This protein has also broad nucleoside diphosphate kinase activity and the activation of protein kinase pathways may be associated with environmental stress and inflammation. However, only the lower concentrations of TiO_2 NPs tested seemed to induce effects in this protein.

4.3.2. Silver NPs

As a consequence of the decreased bioavailability of silver with increased ionic strength of the water, fish inhabiting freshwater environments are more susceptible to silver toxicity compared with marine fish species (Aerle et al., 2013). Nevertheless, some responses were observed in our study that deserve attention.

The action of Ag NPs as antibacterial agents results from the continuous release of silver ions and their ability to increase cell membrane permeability (Kędziora et al., 2018; Yin et al., 2020). While inside

the pathogen cells, the free silver ions can additionally deactivate respiratory enzymes, interrupting ATP production and generating reactive oxygen species (ROS) which prevent deoxyribonucleic acid (DNA) replication and altogether may contribute to cell death (Yin et al., 2020). In the case of eukaryotic cells, different actions of silver ions in cell membranes are reported (Kruszewski et al., 2011; Zhang et al., 2016b; Garuglieri et al., 2018). The Ag NPs may decrease some inflammatory cytokines, leading to anti-inflammatory responses. However, in certain conditions, the Ag NPs are reported to induce ROS generation, leading to cell membrane disruption and DNA modification. The interaction of silver ions with the sulfur and phosphorus of DNA can cause problems in DNA replication and eventually lead to the death of microorganisms (Yin et al., 2020). In our study, functions related with cell structure were revealed; moreover, proteins related with apoptosis were also identified in low extent. Notably, several changes were observed at the proteomic level, in kidney and liver tissues, which align with the previous evidences of the action of Ag NPs in the biological membranes. Our results point to changes in several membrane functions namely, synaptic transmission, vesicle-mediated transport, endocytosis, intracellular trafficking, protein transport and insertion into mitochondrial inner membrane, transmembrane transport and mitochondria fission. The effects of the free silver ions on membrane permeability could, indeed, explain part of the alterations observed at the proteomic level and in the mentioned molecular processes. We cannot discard as well, the hypothetical interaction of the nanoparticles themselves with the biological membranes. Likewise, this interaction has been shown to affect cell viability and also increase membrane permeability (Bannunah et al., 2014). Furthermore, NPs internalization is thought to involve mechanisms of phagocytosis, micropinocytosis, endocytosis, direct diffusion, or adhesive interactions (Wu et al., 2019). These processes presuppose a close interaction of NPs at the molecular level with biological membranes. In the case of Ag NPs, internalization may occur via clathrin-mediated endocytosis (Wu et al., 2019). Size and surface charge are two factors that determine the bioactivity of NPs and their interaction with biological membranes (Bannunah et al., 2014).

Our results showed a dose-dependent effect of PVP-15 nm Ag NPs - which is in agreement with previous studies (e.g.: Aerle et al., 2013; Ferdous Z. and Nemmar A., 2020) since the increase in NPs concentration led to an increase in the number of DEPs in both tissues. Previous works reported that the effects of Ag NPs with size range between 5 nm and 45 nm included alterations on the cell energetic processes (e.g.: Chen et al., 2014; Lee et al., 2015). In our study, the results also suggest alterations induced by Ag NPs exposure on energy/metabolic-related processes on the two analysed tissues. In Chen et al. (2014), a decline in cellular ATP synthesis and attenuation of respiratory chain function was reported. Additionally, these authors reported that cellular energy homeostasis was switched from oxidative phosphorylation-based aerobic metabolism to anaerobic glycolysis (without ROS production). Another work has also reported significant alterations in oxidative phosphorylation and protein synthesis (Aerle et al., 2013). In our work, alterations in oxidative phosphorylation and amino sugar and nucleotide sugar metabolism were suggested in kidney (*lower* concentration). The functional analysis from *lower* Ag NPs concentration also suggested alterations in proteins related with alternative energetic processes, namely synthesis and degradation of ketone bodies and butanoate metabolism. The presence of lipid-derived molecules was previously reported in urine of female rats after exposure to Ag NPs, suggesting effects on excretory function (Razavian and Masaimanesh, 2014). The butanoate, which has a role in lipid metabolism, was also suggested in kidney (*lower* concentration). The nutritional status and the lipid metabolism are important for the immune response and alterations in immune system by Ag NPs have been previously suggested to modulate the microbiota (Lamas et al., 2020). Previous works also reported that Ag (both NPs and ions) affects the mitochondrial respiratory chain of highly energetic demanding organs, such as liver (Almofti et al., 2003, Costa et al., 2010). Oxidative phosphorylation (a term that resulted from the STRING interaction of genes in turbot kidney) is a critical metabolic process to produce energy (ATP) in the cells, requiring the action of respiratory enzyme complexes located in the mitochondrial membrane. The mitochondrial respiratory chain is vulnerable to damage by ROS, and Ag NPs may injure cells by oxidizing the thiol groups of important cell membrane proteins (Costa et al., 2010). Changes in membrane permeability and disruption of mitochondrial functions, as well as, depletion of antioxidant defence mechanisms will lead to oxidative stress (Costa et al., 2010). Altogether, our results are in agreement with the fact that an alteration on energetic balances may occur in turbots exposed to Ag NPs.

Functional analysis also revealed proteins associated with ribosome in liver and kidney. The effect of Ag NPs on protein synthesis of turbot tissues has already been reported previously by Kędziora et al. (2018) and Yin et al. (2020). Those authors explained the ability of silver ions to inhibit the synthesis of proteins by denaturing ribosomes in the cytoplasm. Since the antibacterial toxicity of silver ions is connected with their interaction with structural and functional proteins, the binding of silver ions to ribosomal proteins results in the denaturation of the ribosome native structure and inhibition of protein biosynthesis. The altered functions on ribosomes should be particularly assessed since they can be associated with growth impairment and tumour predisposition (Lai et al., 2009) - although it was not observed in our work along the 14-day exposure. Along with the molecular disturbances in the function of ribosomes, other effects can be expected at the protein level. The results show that Ag NPs may interact with protein folding mechanisms and protein ubiquitination and degradation via ubiquitin pathway. Disturbances in these pathways could be critical to other cellular processes.

A remark should also be given to the type of coating used in the trial with Ag NPs. The PVP coating has been recommended for exposure studies since it provides colloidal stability to Ag NPs, and contributes to even the shape of NPs, reducing aggregation (Tejamaya et al., 2012). Holland et al. (2015) studied the effects of several Ag NPs sizes and coatings on serum cytokines and additional cardiac endpoints in rats after pulmonary exposure. These authors found that acute effects were coating-independent; however, the persistence of injury was greater for 110 nm PVP-Ag NPs than using other coatings (and different NPs sizes) possibly due to the increased stability of the NPs. In a different work, Ferdous et al. (2018) showed that different capping (citrate vs PVP) equally causes adverse effects on mice erythrocytes. On one hand, such works revealed the wide range of toxic effects of Ag NPs, but they also highlight the complexity of studying such compounds, with such high diverse or potential diverse properties.

Finally, we highlight the impact of Ag NPs in several kinases and proteins with functions in cell signalling since they play a critical role in cells (interacting with other proteins, and regulating their activity and functions in multiple processes).

4.3.3. Candidate protein markers of nanoparticles exposure

Among the 114 DEPs identified, we selected 21 proteins as candidate biomarkers for exposure to citrate P25 TiO_2 and PVP 15 nm Ag NPs, based on their altered protein expression in both NPs concentrations groups when compared to control group (Table 2).

At the TiO_2 NPs trial, three proteins had significantly altered expression levels at both *lower* and *higher* TiO_2 NPs groups in turbot liver in comparison to untreated control samples, including *serpina7*, which has a role as serpin peptidase inhibitor and negative regulation of endopeptidase activity. At the Ag NPs trial, three proteins were differentially expressed in liver with both *lower* and *higher* concentrations of Ag NPs, including adaptor-related protein complex 1, beta 1 subunit, which is important for endocytosis and protein transport and deoxyribose-phosphate aldolase, with a role on metabolic pathways expression. In addition, in Ag NPs trial 15 proteins were differentially expressed in kidney at both tested concentrations, including proteins with roles on biosynthesis of amino acids, metabolic pathways or

Table 2
Candidate proteins for use as exposure biomarkers of TiO_2 and Ag NPs. ↑ Denotes up-regulation of proteins as result of the exposure to both concentrations tested. ↓ Denotes down-regulation of proteins as result of the exposure to both concentrations tested.

#	Accession number	Protein name	Gene	Biological function	Response to exposure	
					TiO_2 NPs	Ag NPs
1	A0A2U9C4V6	FAT atypical cadherin 2	*fat2*	Calcium ion binding	Liver ↓	–
2	A0A6A4T4Q5	Microfibrillar-associated protein 4	*mfap4*	Antigen binding Carbohydrate derivative binding Signaling receptor binding	Liver ↓	–
3	A0A2U9BTR1	Serpin peptidase inhibitor, clade A (alpha-1 antiproteinase, antitrypsin), member 7	*serpina7*	Major thyroid hormone transport protein in serum Serine-type endopeptidase inhibitor activity Negative regulation of endopeptidase activity	Liver ↑	–
4	A0A2U9BU90	Adaptor-related protein complex 1, beta 1 subunit	*ap1b1*	Endocytosis Protein transport	–	Liver ↑
5	A0A2U9CD78	Splicing factor 3b, subunit 1	*sf3b1*	Spliceosome	–	Liver ↑
6	A0A2U9BAV2	Deoxyribose-phosphate aldolase (putative)	*dera*	Metabolic pathways	–	Liver ↑
7	A0A2U9BHN3	acyl-CoA dehydrogenase family, member 9	*acad9*	Fatty acid metabolism Oxidative phosphorylation	–	Kidney ↑
8	A0A2U9AXB9	Apolipoprotein A-IV b, tandem duplicate 2	*apoa4b.2*	Lipid binding and transport Lipoprotein metabolic processes	–	Kidney ↑
9	A0A2U9CHX2	argininosuccinate synthase	*ass1*	Biosynthesis of aminoacids Metabolic pathways	–	Kidney ↑
10	A0A2U9BE63	C-src tyrosine kinase	*csk*	Regulation of cell growth differentiation and migration Immune response	–	Kidney ↑
11	A0A2U9CUV9	Cytochrome P450, family 2, subfamily k, polypeptide 21	*cyp2k21*	Oxidative metabolism of xenobiotics Metabolism of various endogenous substrates	–	Kidney ↑
12	A0A2U9C4F6	Peptidylprolyl isomerase	*fkbp2*	Immuno-regulation and basic cellular processes involving protein folding and trafficking	–	Kidney ↑
13	A0A2U9AXL7	Flotillin 1	*flot1b*	Vesicle trafficking and cell morphology	–	Kidney ↑
14	A0A6A4T510	Guanine nucleotide-binding protein subunit beta-2-like 1	*gnb2l1*	Protein kinase C binding Ribosome binding	–	Kidney ↑
15	A0A2U9BL92	NADH dehydrogenase (ubiquinone) 1 beta subcomplex, 3	*ndufb3*	Electron transport Respiratory chain Transport	–	Kidney ↑
16	A0A2U9AXC7	Platelet-activating factor acetylhydrolase, isoform Ib, gamma subunit	*pafah1b3*	Lipid metabolism Metabolic pathways	–	Kidney ↓
17	A0A2U9CF06	Surfactant protein Bb	*sftpbb*	**N/A**	–	Kidney ↑
18	A0A2U9BGN8	Sorting nexin-5/6/32	*si:dkey-28n18.9*	Membrane trafficking	–	Kidney ↑
19	A0A2U9B8B5	S-phase kinase-associated protein 1	*skp1*	Ubiquitin system	–	Kidney ↑
20	A0A6A4TX03	Syntaxin 12, like	*stx12l*	intracellular protein transport	–	Kidney ↑
21	A0A6A4T3P3	Mitochondrial import inner membrane translocase subunit	*timm13*	Transport of proteins into the mitochondria	–	Kidney ↑

oxidative phosphorylation (such as argininosuccinate synthase, putative NADH dehydrogenase, and C-src tyrosine kinase, among others). In addition, proteins related with xenobiotic and environmental adaptation (such as Cytochrome P450, family 2, subfamily k, polypeptide 21) are also suggested.

5. Conclusions

In our work, the overall evaluation of alterations studied in liver and kidney of turbot juveniles, suggests a wider range of responses induced by Ag NPs when compared to TiO_2 NPs. Although clear acute toxicity was not evident in any of the NPs studies, molecular alterations may culminate as toxic effects and physiological harm in the long term, and their release to the aquatic environment should be avoided by precaution. In the case of TiO_2 NPs exposure, the extent of the metabolic effects observed (e.g.: lipid and energy metabolism-related processes, lipid droplets coalescence, decreased fish growth) deserves further study. In the case of Ag NPs, effects in several molecular processes (inc. metabolism) are also suggested and therefore, the use of these NPs for specific biological applications should be further assessed to understand and balance their advantages (e.g. protective action against infectious diseases) or disadvantages (e.g.: ribosome functioning alterations and inhibition of protein biosynthesis, that may lead to effects at cellular level).

Author Statement

Conceptualization, JCM,AC,SC,BE,PBB, Methodology, MJA,MLS,EF, ABF,MV,MO, NM,LRL,MQ,IP,MVT,JJLM,EPV,MCBA,MSC, Writing – original draft, MJA,MLS, Writing – review & editing, EF,ABF,MV,NM, MVT,MO,LRL,EPV,AC, Supervision, JCM,SC,BE,VV,AC,PBB, Funding acquisition, BE,VV,AC,PBB,SC.

Declaration of competing interest

The authors declare that they have no known competing financial interests or personal relationships that could have appeared to influence the work reported in this paper.

Data availability

The mass spectrometry proteomics data have been deposited to the ProteomeXchange Consortium via the PRoteomics IDEntifications (PRIDE) Archive repository with the dataset identifier PXD037420.

Additional data will be made available on request.

Acknowledgements

This research was funded by the European Regional Development Fund (ERDF) through Interreg Atlantic Area Program, project NANOCULTURE (reference EAPA 590/2018) and in the framework of the program PT2020, and UIDB/04423/2020 and UIDP/04423/2020, through national funds provided by Portuguese Foundation for Science and Technology (Fundação para a Ciência e Tecnologia; FCT). We thank the Nanophotonics & Bioimaging and AEMIS facilities and staff at INL and Centre for Scientific and Technological Support to Research (CACTI) at University of Vigo for their contribution. Mass spectrometry analysis was carried out at the Mass Spectrometry Core Facility of Faculty of Medicine and Health Sciences, Linköping University, Sweden. The authors would like to acknowledge the comments of two anonymous reviewers.

Appendix A. Supplementary data

Supplementary data to this article can be found online at https://doi.org/10.1016/j.chemosphere.2022.136110.

References

Abbas, Q., Yousaf, B., Amina, Ali M.U., Munir, M.A.M., El-Naggar, A., Rinklebe, J., Naushad, M., 2020. Transformation pathways and fate of engineered nanoparticles (ENPs) in distinct interactive environmental compartments: a review. Environ. Int. 138, 105646 https://doi.org/10.1016/j.envint.2020.105646.

Aerle, R., Lange, A., Moorhouse, A., Paszkiewicz, K., Ball, K., Johnston, B.D., Bastos, E., Booth, T., Tyler, C.R., Santos, E.M., 2013. Molecular mechanisms of toxicity of silver nanoparticles in zebrafish embryos. Environ. Sci. Technol. 47 (14), 8005–8014. https://doi.org/10.1021/es401758d.

Almofti, M.R., Ichikawa, T., Yamashita, K., Terada, H., Shinohara, Y., 2003. Silver ion induces a cyclosporine a-insensitive permeability transition in rat liver mitochondria and release of apoptogenic cytochrome C. J. Biochem. 134 (1), 43–49. https://doi.org/10.1093/jb/mvg111.

Amde, M., Liu, J., Tan, Z.-Q., Bekana, B., 2017. Transformation and bioavailability of metal oxide nanoparticles in aquatic and terrestrial environments. A review. Environ. Pollut. 230, 250–267. https://doi.org/10.1016/j.envpol.2017.06.064.

ANSES, 2019. Avis de l'Agence nationale de sécurité sanitaire de l'alimentation, de l'environnement et du travail relatif au risques liés à la ingestion de l'additif alimentaire E 171. Saisine n° 2019-SA-0036. Available online: https://www.anses.fr/fr/system/files/ERCA201.

Araújo, M.J., Sousa, M.L., Felpeto, A.B., Turkina, M.V., Fonseca, E., Martins, J.C., Vasconcelos, V., Campos, A., 2021. Comparison of sample preparation methods for shotgun proteomic studies in aquaculture species. Proteomes 9, 46. https://doi.org/10.3390/proteomes9040046.

Asztemborska, M., Jakubiak, M., Stęborowski, R., Chajduk, E., Bystrzejewska-Piotrowska, G., 2018. Titanium dioxide nanoparticle circulation in an aquatic ecosystem. Water Air Soil Pollut. 229 (6), 208. https://doi.org/10.1007/s11270-018-3852-8.

Auclair, J., Turcotte, P., Gagnon, C., Peyrot, C., Wilkinson, K.J., Gagné, F., 2019. The influence of surface coatings on the toxicity of silver nanoparticle in rainbow trout. Comp. Biochem. Physiol. C Toxicol. Pharmacol. 226, 108623 https://doi.org/10.1016/j.cbpc.2019.108623.

Auría-Soro, C., Nesma, T., Juanes-Velasco, P., Landeira-Viñuela, A., Fidalgo-Gomez, H., Acebes-Fernandez, V., Gongora, R., Almendral Parra, M.J., Manzano-Roman, R., Fuentes, M., 2019. Interactions of nanoparticles and biosystems: microenvironment of nanoparticles and biomolecules in nanomedicine. Nanomaterials 9 (10), 1365. PMC6835394 10.3390/nano9101365. PMID: 31554176.

Austin, L.A., Mackey, M.A., Dreaden, E.C., El-Sayed, M.A., 2014. The optical, photothermal, and facile surface chemical properties of gold and silver nanoparticles in biodiagnostics, therapy, and drug delivery. Arch. Toxicol. 88 (7), 1391–1417. https://doi.org/10.1007/s00204-014-1245.

Aznar, R., Barahona, F., Geiss, O., Ponti, J., Luis, T.J., Barrero-Moreno, J., 2017. Quantification and size characterisation of silver nanoparticles in environmental aqueous samples and consumer products by single particle-ICPMS. Talanta 175, 200–208. https://doi.org/10.1016/j.talanta.2017.07.048.

Bannunah, A.M., Vllasaliu, D., Lord, J., Stolnik, S., 2014 Dec 1. Mechanisms of nanoparticle internalization and transport across an intestinal epithelial cell model: effect of size and surface charge. Mol. Pharm. 11 (12), 4363–4373. https://doi.org/10.1021/mp500439c.

Baranowska-Wójcik, E., Szwajgier, D., Oleszczuk, P., Winiarska-Mieczan, A., 2020. Effects of titanium dioxide nanoparticles exposure on human health-a review. Biol. Trace Elem. Res. 193 (1), 118–129. https://doi.org/10.1007/s12011-019-01706-6.

Bartucci, R., Paramanandana, A., Boersma, Y.L., Olinga, P., Salvati, A., 2020. Comparative study of nanoparticle uptake and impact in murine lung, liver and kidney tissue slices. Nanotoxicology 14 (6), 847–865. https://doi.org/10.1080/17435390.2020.1771785.

Bäuerlein, P.S., Emke, E., Tromp, P., Hofman, J.A.M.H., Carboni, A., Schooneman, F., de Voogt, P., van Wezel, A.P., 2017 Jan 15. Is there evidence for man-made nanoparticles in the Dutch environment? Sci. Total Environ. 576, 273–283. https://doi.org/10.1016/j.scitotenv.2016.09.206. Epub 2016 Oct 24. PMID: 27788442.

Biswas, J.K., Sarkar, D., 2019. Nanopollution in the aquatic environment and ecotoxicity: No nano issue. Curr. Pollut. Rep. 5, 4–7. https://doi.org/10.1007/s40726-019-0104-5.

Boletín Oficial del Estado (BOE), 2013. Real Decreto (R.D.) 53/2013, de 1 de febrero, por el que se establecen las normas básicas aplicables para la protección de los animales utilizados en experimentación y otros fines científicos, incluyendo la docencia - 'Royal Decree (R.D.) 53/2013, of February 1, which establishes the basic applicable standards for the protection of animals used in experimentation and other scientific purposes, including teaching' (in Spanish). BOE 34, 8/Feb/2013: 11370-11421, p. 52. Secction 1, BOE-A-2013-1337.

Brand, W., Peters, R.J.B., Braakhuis, H.M., Maślankiewicz, L., Oomen, A.G., 2020. Possible effects of titanium dioxide particles on human liver, intestinal tissue, spleen and kidney after oral exposure. Nanotoxicology 14 (7), 985–1007. https://doi.org/10.1080/17435390.2020.1778809.

Briffa, J., Sinagra, E., Blundell, R., 2020. Heavy metal pollution in the environment and their toxicological effects on humans. Heliyon 6 (9), e04691. https://doi.org/10.1016/j.heliyon.2020.e04691.

Bundschuh, M., Filser, J., Lüderwald, S., et al., 2018. Nanoparticles in the environment: where do we come from, where do we go to? Environ. Sci. Eur. 30, 6. https://doi.org/10.1186/s12302-018-0132-6.

Campos, A., Tedesco, S., Vasconcelos, V., Cristobal, S., 2012 Jul 19. Proteomic research in bivalves: towards the identification of molecular markers of aquatic pollution. J Proteomics 75 (14), 4346–4359. https://doi.org/10.1016/j.jprot.2012.04.027. Epub 2012 May 2. PMID: 22579653.

Campos, A., Apraiz, I., da Fonseca, R.R., Cristobal, S., 2015. Shotgun Analysis of the Marine Mussel Mytilus Edulis Hemolymph Proteome and Mapping the Innate Immunity Elements. Proteomics15, pp. 4021–4029.

Campos, A., Danielsson, G., Farinha, A.P., Kuruvilla, J., Warholm, P., Cristobal, S., 2016. Shotgun proteomics to unravel marine mussel (*Mytilus edulis*) response to long-term exposure to low salinity and propranolol in a Baltic Sea microcosm. J. Proteonomics 137, 97–106.

Cao, X., Han, Y., Gu, M., Du, H., Song, M., Zhu, X., Ma, G., Pan, C., Wang, W., Zhao, E., Goulette, T., Yuan, B., Zhang, G., Xiao, H., 2020. Foodborne titanium dioxide nanoparticles induce stronger adverse effects in obese mice than non-obese mice: gut microbiota dysbiosis, colonic inflammation, and proteome alterations. Small 16 (36), e2001858. https://doi.org/10.1002/smll.202001858.

Carmo, T.L.L., Siqueira, P.R., Azevedo, V.C., Tavares, D., Pesenti, E.C., Cestari, M.M., Martinez, C.B.R., Fernandes, M.N., 2019. Overview of the toxic effects of titanium dioxide nanoparticles in blood, liver, muscles, and brain of a Neotropical detritivorous fish. Environ. Toxicol. 34 (4), 457–468, 10.1002/tox.22699. MID: 30604913.

Carvalhais, A., Pereira, B., Sabato, M., Seixas, R., Dolbeth, M., Marques, A., Guilherme, S., Pereira, P., Pacheco, M., Mieiro, C., 2021. Mild effects of sunscreen agents on a marine flatfish: oxidative stress, energetic profiles, neurotoxicity and behaviour in response to titanium dioxide nanoparticles and oxybenzone. Int. J. Mol. Sci. 4 (22), 1567. https://doi.org/10.3390/ijms22041567. PMID: 33557180.

Causey, D.R., Pohl, M.A.N., Stead, D.A., Martin, S.A.M., Secombes, C.J., Macqueen, D.J., 2018. High-throughput proteomic profiling of the fish liver following bacterial infection. BMC Genom. 19 (1), 719. https://doi.org/10.1186/s12864-018-5092-0.

Chan, P.P., Wasinger, V.C., Leong, R.W., 2016. Current application of proteomics in biomarker discovery for inflammatory bowel disease. World J. Gastrointest. Pathophysiol. 7 (1), 27–37. https://doi.org/10.4291/wjgp.v7.i1.27.

Chen, Y., Wang, Z., Xu, M., Wang, X., Liu, R., Liu, Q., Zhang, Z., Xia, T., Zhao, J., Jiang, G., Xu, Y., Liu, S., 2014. Nanosilver incurs an adaptive shunt of energy metabolism mode to glycolysis in tumor and nontumor cells. ACS Nano 8 (6), 5813–5825. https://doi.org/10.1021/nn500719m.

Chow, J.C.L., 2021. Additive Manufacturing with Functionalized Nanomaterials - synthesis and applications of functionalized nanoparticles in biomedicine and radiotherapy. Micro Nano Technol. 193–218. https://doi.org/10.1016/B978-0-12-823152-4.00001-6.

Cichoż-Lach, H., Michalak, A., 2014. Oxidative stress as a crucial factor in liver diseases. World J. Gastroenterol. 20 (25), 8082–8091. https://doi.org/10.3748/wjg.v20.i25.8082.

Costa, C.S., Ronconi, J.V.V., Daufenbach, J.F., Gonçalves, C.L., Rezin, G.T., Streck, E.L., Paula, M.M., 2010. In vitro effects of silver nanoparticles on the mitochondrial respiratory chain. Mol. Cell. Biochem. 342, 51–56. https://doi.org/10.1007/s11010-010-0467-9.

Dawadi, S., Katuwal, S., Gupta, A., Lamichhane, U., Thapa, R., Jaisi, S., Lamichhane, G., Bhattarai, D.P., Parajuli, N., 2021. Current research on silver nanoparticles: synthesis, characterization, and applications. J. Nanomater., 6687290 https://doi.org/10.1155/2021/6687290.

Dedman, C., King, A.M., Christie-Oleza, J.A., Davies, G.-M., 2021. Environmentally relevant concentrations of titanium dioxide nanoparticles pose negligible risk to marine microbes. Environ. Sci.: Nano 8, 1236–1255. https://doi.org/10.1039/D0EN00883D.

Dhupal, M., Oh, J.M., Tripathy, D.R., Kim, S.K., Koh, S.B., Park, K.S., 2018. Immunotoxicity of titanium dioxide nanoparticles via simultaneous induction of apoptosis and multiple toll-like receptors signaling through ROS-dependent SAPK/JNK and p38 MAPK activation. Int. J. Nanomed. 13, 6735–6750. https://doi.org/10.2147/IJN.S176087. PMID: 30425486; PMCID: PMC6204851.

European Food Safety Authority (EFSA), 2016. Scientific opinion on the re-evaluation of silver (E 174) as food additive. EFSA J. 14 (1), 4364.
European Food Safety Authority (EFSA), 2021. Scientific Opinion - safety assessment of titanium dioxide (E171) as a food additive. EFSA J. 19 (5), e06585 https://doi.org/10.2903/j.efsa.2021.6585.
European Market Observatory for Fisheries and Aquaculture Products (EUMOFA), 2018. Turbot in the EU. Directorate-General for Maritime Affairs and Fisheries of the European Commission. Brussels., p 43. https://doi.org/10.2771/763683
European Union (EU), 2010. Directive 2010/63/EU of the EUROPEAN PARLIAMENT and of the COUNCIL on the Protection of Animals Used for Scientific Purposes. Official Journal of the European Union L 276, pp. 33–79.
Felice, B.D., Parolini, M., 2020. Can proteomics Be considered as a valuable tool to assess the toxicity of nanoparticles in marine bivalves? J. Mar. Sci. Eng. 8 (12), 1033. https://doi.org/10.3390/jmse8121033.
Ferdous, Z., Nemmar, A., 2020. Health impact of silver nanoparticles: a review of the biodistribution and toxicity following various routes of exposure. Int. J. Mol. Sci. 21 (7), 2375. https://doi.org/10.3390/ijms21072375.
Ferdous, Z., Beegam, S., Tariq, S., Ali, B.H., Nemmar, A., 2018. The in vitro effect of polyvinylpyrrolidone and citrate coated silver nanoparticles on erythrocytic oxidative damage and eryptosis. Cell. Physiol. Biochem. 49 (4), 1577–1588. https://doi.org/10.1159/000493460.
Food and Agriculture Organization (FAO), 2022. Fisheries and aquaculture - national aquaculture sector overview, Spain. Fisheries and Aquaculture Division [online]. Rome. [Cited Wednesday, May 18th 2022]. https://www.fao.org/fishery/en/countrysector/es/en.
Garuglieri, E., Meroni, E., Cattò, C., Villa, F., Cappitelli, F., Erba, D., 2018. Effects of sub-lethal concentrations of silver nanoparticles on a simulated intestinal prokaryotic-eukaryotic interface. Front. Microbiol. 8, 2698. https://doi.org/10.3389/fmicb.2017.02698.
Ge, Y., Bruno, M., Wallace, K., Winnik, W., Prasad, R.Y., 2011. Proteome profiling reveals potential toxicity and detoxification pathways following exposure of BEAS-2B cells to engineered nanoparticle titanium dioxide. Proteomics 11 (12), 2406–2422. https://doi.org/10.1002/pmic.201000741.
Giese, B., Klaessig, F., Park, B., et al., 2018. Risks, release and concentrations of engineered nanomaterial in the environment. Sci. Rep. 8, 1565. https://doi.org/10.1038/s41598-018-19275-4.
Gluchowski, N.L., Becuwe, M., Walther, T.C., Farese Jr., R.V., 2017. Lipid droplets and liver disease: from basic biology to clinical implications. Nat. Rev. Gastroenterol. Hepatol. 14 (6), 343–355. https://doi.org/10.1038/nrgastro.2017.32.
Grasso, A., Ferrante, M., Arena, G., Salemi, R., Zuccarello, P., Fiore, M., Copat, C., 2021. Chemical characterization and quantification of silver nanoparticles (Ag-NPs) and dissolved Ag in seafood by single particle ICP-MS: assessment of dietary exposure. Int. J. Environ. Res. Publ. Health 18 (8), 4076. https://doi.org/10.3390/ijerph18084076.
Handy, R.D., Henry, T.B., Scown, T.M., et al., 2008. Manufactured nanoparticles: their uptake and effects on fish—a mechanistic analysis. Ecotoxicology 17, 396–409. https://doi.org/10.1007/s10646-008-0205-1.
Helmlinger, J., Sengstock, C., Groß-Heitfeld, C., Mayer, C., Schildhauer, T.A., Köllerb, M., Epple, M.M., 2016. Silver nanoparticles with different size and shape: equal cytotoxicity, but different antibacterial effects. RSC Adv. 6, 18490–18501. https://doi.org/10.1039/C5RA27836H.
Holland, N.A., Thompson, L.C., Vidanapathirana, A.K., Urankar, R.N., Lust, R.M., Fennell, T.R., Wingard, C.J., 2015. Impact of pulmonary exposure to gold core silver nanoparticles of different size and capping agents on cardiovascular injury. Part. Fibre Toxicol. 13, 48. https://doi.org/10.1186/s12989-016-0159-z.
Hughes, C.S., Moggridge, S., Müller, T., Sorensen, P.H., Morin, G.B., Krijgsveld, J., 2019. Single-pot, solid-phase-enhanced sample preparation for proteomics experiments. Nat. Protoc. 14 (1), 68–85. https://doi.org/10.1038/s41596-018-0082-x. PMID: 30464214.
IARC Working, 2010. Group on the evaluation of carcinogenic risks to humans. In: International Agency for Research on Cancer and World Health Organization. International Agency for Research on Cancer, Distributed by WHO Press, Lyon, France, Geneva. Carbon black, titanium dioxide, and talc.
Ivanova, N., Gugleva, V., Dobreva, M., Pehlivanov, I., Stefanov, S., Andonova, V., 2018. Silver nanoparticles as multi-functional drug delivery systems. In: Nanomedicines. IntechOpen, London, UK.
Janković, N.Z., Plata, D.L., 2019. Engineered nanomaterials in the context of global element cycles. Environ. Sci.: Nano 6, 2697–2711. https://doi.org/10.1039/c9en00322c.
Jovanović, B., Whitley, E.M., Kimura, K., Crumpton, A., Palić, D., 2015. Titanium dioxide nanoparticles enhance mortality of fish exposed to bacterial pathogens. Environ. Pollut. 203, 153–164. https://doi.org/10.1016/j.envpol.2015.04.003. PMID: 25884347.
Kędziora, A., Speruda, M., Krzyżewska, E., Rybka, J., Łukowiak, A., Bugla-Płoskońska, G., 2018. Similarities and differences between silver ions and silver in nanoforms as antibacterial agents. Int. J. Mol. Sci. 19 (2), 444. https://doi.org/10.3390/ijms19020444. PMID: 29393866; PMCID: PMC5855666.
Khalil, A., Fizree, H.M., Jawaid, M., Alattas, O.S., 2011. Preparation and characterization of nano-structured materials from oil palm ash: a bioagricultural waste from oil palm mill. Bioresources 6 (4), 4537–4546.
Khan, I., Saeed, K., Khan, I., 2019. Nanoparticles: properties, applications and toxicities. Arab. J. Chem. 12 (7), 908–931. https://doi.org/10.1016/j.arabjc.2017.05.011.
Khosravi-Katuli, K., Prato, E., Lofrano, G., Guida, M., Vale, G., Libralato, G., 2017. Effects of nanoparticles in species of aquaculture interest. Environ. Sci. Pollut. Res. Int. 24 (21), 17326–17346. https://doi.org/10.1007/s11356-017-9360-3. PMID: 28597390.
Kim, M.-S., Louis, K.M., Pedersen, J.A., Hamers, R.J., Peterson, R.E., Heideman, W., 2014. Using citrate-functionalized TiO_2 nanoparticles to study the effect of particle size on zebrafish embryo toxicity. Analyst 139, 964–972. https://doi.org/10.1039/C3AN01966G.
Koo, J.H., 2006. Polymer Nanocomposites: Processing, Characterization, and Applications. McGraw-Hill.
Kose, Ozge, Stalet, Marion, Leclerc, Lara, Forest, Valérie, 2020. Influence of the physicochemical features of TiO 2 nanoparticles on the formation of a protein corona and impact on cytotoxicity. RSC Adv. Royal Soc. Chem. 10 (72), 43950–43959 ff10.1039/d0ra08429hff. ffhal-03066132f.
Kruszewski, M., Brzoska, K., Brunborg, G., Asare, N., Dobrzynska, M., Dusinska, M., Fjellsbø, L.M., Georgantzopoulou, A., Gromadzka-ostrowska, J., Gutleb, A.C., Lankoff, A., Pran, E.R., Rinna, A., Instanes, C., Sandberg, W.J., Schwarze, P., Tomasz, S., Wojewodzka, M., Refnes, M., 2011. Toxicity of silver nanomaterials in higher eukaryotes. Adv. Mol. Toxicol. 179–2018, 10.1016/B978-0-444-53864-2.00005-0.
Lai, K., Amsterdam, A., Farrington, S., Bronson, R.T., Hopkins, N., Lees, J.A., 2009. Many ribosomal protein mutations are associated with growth impairment and tumor predisposition in zebrafish. In: Dev Dyn, vol. 238. PMCID, pp. 76–85. https://doi.org/10.1002/dvdy.21815. PMID: 19097187.
Lamas, B., Breyner, N.M., Houdeau, E., 2020. Impacts of foodborne inorganic nanoparticles on the gut microbiota-immune axis: potential consequences for host health. Part. Fibre Toxicol. 17, 19.
Lee, M.J., Lee, S.J., Yun, S.J., Jang, J.Y., Kang, H., Kim, K., Choi, I.H., Park, S., 2015. Silver nanoparticles affect glucose metabolism in hepatoma cells through production of reactive oxygen species. Int. J. Nanomed. 11, 55–68. https://doi.org/10.2147/IJN.S94907. PMID: 26730190; PMCID: PMC4694681.
Li, D., Chan, D.W., 2014. Proteomic cancer biomarkers from discovery to approval: it's worth the effort. Expert Rev. Proteomics 11 (2), 135–136, 10.1586/14789450.2014.897614. PMID: 24646122.
Liu, J., Hurt, R.H., 2010. Ion release kinetics and particle persistence in aqueous nano-silver colloids. Environ. Sci. Technol. 44 (6), 2169–2175. https://doi.org/10.1021/es9035557.
Lückstädt, C., 2008. The use of acidifiers in fish nutrition. CAB reviews: perspectives in agriculture, veterinary science. Nutr. Nat. Res. 3 (44) https://doi.org/10.1079/PAVSNNR20083044.
Lynch, Dawson, 2008. Protein-nanoparticle interactions. Nano Today 3 (1), 40–47. https://doi.org/10.1016/S1748-0132(08)70014-8.
Madanayake, N.H., Perera, N., Adassooriya, N.M., 2022. Engineered nanomaterials: threats, releases, and concentrations in the environment. In: Sarma, Hemen, Delfina, C., Dominguez, Lee, Wen-Yee (Eds.), Emerging Contaminants in the Environment. Elsevier, ISBN 9780323851602, pp. 225–240. https://doi.org/10.1016/B978-0-323-85160-2.00001-9.
Martínez-Reyes, I., Chandel, N.S., 2020. Mitochondrial TCA cycle metabolites control physiology and disease. Nat. Commun. 11, 102. https://doi.org/10.1038/s41467-019-13668-3.
Martins, J.C., Domínguez-Pérez, D., Azevedo, C., Braga, A.C., Costa, P.R., Osório, H., Vasconcelos, V., Campos, A., 2020. Molecular responses of mussel Mytilus galloprovincialis associated to accumulation and depuration of marine biotoxins okadaic acid and dinophysistoxin-1 revealed by shotgun proteomics. Front. Mar. Sci. 7, 1101.
Meena, R., Paulraj, R., 2012. Oxidative stress mediated cytotoxicity of TiO_2 nano anatase in liver and kidney of Wistar rat. Toxicol. Environ. Chem. 94 (1) https://doi.org/10.1080/02772248.2011.638441.
Moore, T., Rodriguez-Lorenzo, L., Hirsch, V., Balog, S., Urban, D., Jud, C., Rothen-Rutishauser, B., Lattuada, M., Petri-Fink, A., 2015. Nanoparticle colloidal stability in cell culture media and impact on cellular interactions. Chem. Soc. Rev. 44, 6287–6305.
Musial, J., Krakowiak, R., Mlynarczyk, D.T., Goslinski, T., Stanisz, B.J., 2020. Titanium dioxide nanoparticles in food and personal care products-what do we know about their safety? Nanomaterials 10 (6), 1110. https://doi.org/10.3390/nano10061110. PMID: 32512703.
Nesvizhskii, A.I., Keller, A., Kolker, E., Aebersold, R., 2003. A statistical model for identifying proteins by tandem mass spec-trometry. Anal. Chem. 75 (17), 4646–4658.
Pedley, A.M., Benkovic, S.J., 2017. A new view into the regulation of purine metabolism: the purinosome. Trends Biochem. Sci. 42 (2), 141–154. https://doi.org/10.1016/j.tibs.2016.09.009. PMID: 28029518.
Picard, M., McEwen, B.S., Epel, E.S., Sandi, C., 2018. An energetic view of stress: focus on mitochondria. Front. Neuroendocrinol. 49, 72–85. https://doi.org/10.1016/j.yfrne.2018.01.001.
Powers, C.M., Slotkin, T.A., Seidler, F.J., Badireddy, A.R., Padilla, S., 2011. Silver nanoparticles alter zebrafish development and larval behavior: distinct roles for particle size, coating and composition. Neurotoxicol. Teratol. 33 (6), 708–714. https://doi.org/10.1016/j.ntt.2011.02.002. PMID: 21315816.
Quarato, M., Pinheiro, I., Vieira, A., Espiña, B., Rodriguez-Lorenzo, L., 2021. Detection of silver nanoparticles in seawater using surface-enhanced Raman scattering. Nanomaterials 11, 1711. https://doi.org/10.3390/nano11071711.
R Core Team, 2021. R: A Language and Environment for Statistical Computing. R Foundation for Statistical Computing, Vienna, Austria. URL. https://www.R-project.org/.
Razavian, M.H., Masaimanesh, M., 2014. Ingestion of silver nanoparticles leads to changes in blood parameters. Nanomed. J. 1 (5), 339–345.
Rodrigues, P.M., Schrama, D., Campos, A., Osório, H., Freitas, M., 2016. Applications of proteomics in aquaculture. In: Salekdeh, G.H. (Ed.), Agricultural Proteomics Volume

1: Crops, Horticulture, Farm Animals, Food, Insect and Microorganisms. Springer International Publishing, Cham, Denmark, pp. 175–209.
Rodrigues, P.M., Campos, A., Kuruvilla, J., Schrama, D., Cristobal, S., 2017. Chapter 17—proteomics in aquaculture: quality and safety. In: Colgrave, M.L. (Ed.), Proteomics in Food Science. Elsevier, Amsterdam, The Netherlands, pp. 279–295.
Romeu, M.J., Domínguez-Pérez, D., Almeida, D., Morais, J., Araújo, M.J., Osório, H., Campos, A., Vasconcelos, V., Mergulhão, F.J.M., 2021. Quantitative proteomic analysis of marine biofilms formed by filamentous cyanobacterium. Environ. Res. 201, 111566.
Saptarshi, S.R., Duschl, A., Lopata, A.L., 2013. Interaction of nanoparticles with proteins: relation to bio-reactivity of the nanoparticle. J. Nanobiotechnol. 11, 26. https://doi.org/10.1186/1477-3155-11-26.
Schott, M., Weller, S., Schulze, R.J., Krueger, E.W., Drizyte-Miller, K., Casey, C.A., McNiven, M.A., 2019. Lipid droplet size directs lipolysis and lipophagy catabolism in hepatocytes. J. Cell Biol. 218 (10), 3320–3335. https://doi.org/10.1083/jcb.201803153.
Shah, S.Z.H., Afzal, M., Khan, S.Y., Hussain, S.M., Habib, R.Z., 2015. Int. J. Agric. Biol. 17, 1–8. Prospects of using citric acid as fish feed supplement.
Shah, B.R., Mraz, J., 2019. Advances in nanotechnology for sustainable aquaculture and fisheries. Rev. Aquacult. 12 (2), 925–942. https://doi.org/10.1111/raq.12356.
Shakeel, M., Jabeen, F., Qureshi, N.A., Fakhr-E-Alam, M., 2016. Toxic effects of titanium dioxide nanoparticles and titanium dioxide bulk salt in the liver and blood of male sprague-dawley rats assessed by different assays. Biol. Trace Elem. Res. 173 (2), 405–426. https://doi.org/10.1007/s12011-016-0677-4. PMID: 27008428.
Sharma, S., Sharma, R.K., Gaur, K., Cátala Torres, J.F., Loza-Rosas, S.A., Torres, A., Saxena, M., Julin, M., Tinoco, A.D., 2019. Fueling a hot debate on the application of TiO_2 nanoparticles in sunscreen. Materials 12 (14), 2317. https://doi.org/10.3390/ma12142317. PMID: 31330764; PMCID: PMC6678326.
Shi, H., Magaye, R., Castranova, V., et al., 2013. Titanium dioxide nanoparticles: a review of current toxicological data. Part. Fibre Toxicol. 10, 15. https://doi.org/10.1186/1743-8977-10-15.
Silva, P.V., Pinheiro, C., Morgado, R.G., Verweij, R.A., van Gestel, C.A.M., Loureiro, S., 2022. Bioaccumulation but no biomagnification of silver sulfide nanoparticles in freshwater snails and planarians. In: Sci Total Environ, vol. 20, p. 808. https://doi.org/10.1016/j.scitotenv.2021.151956.
Skocaj, M., Filipic, M., Petkovic, J., Novak, S., 2011. Titanium dioxide in our everyday life; is it safe?. In: Radiol Oncol, vol. 45. PMCID, pp. 227–247. https://doi.org/10.2478/v10019-011-0037-0. PMID: 22933961.
Song, B., Zhang, Y., Liu, J., Feng, X., Zhou, T., Shao, L., 2016. Is neurotoxicity of metallic nanoparticles the cascades of oxidative stress? Nanoscale Res. Lett. 11, 291. https://doi.org/10.1186/s11671-016-1508-4.
Sotoudeh, E., Sangari, M., Bagheri, D., Morammazi, S., Mozanzadeh, M.T., 2020. Dietary organic acid salts mitigate plant protein induced inflammatory response and improve humoral immunity, antioxidative status and digestive enzyme activities in yellowfin seabream, Acanthopagrus latus. Aquacult. Nutr. 26 (5), 1669–1680. https://doi.org/10.1111/anu.13112.
Soulliere, C., Dixon, B., 2017. Immune system organs of bony fishes. In: Reference Module in Life Sciences. https://doi.org/10.1016/B978-0-12-809633-8.12179-X.
Stensberg, M.C., Wei, Q., McLamore, E.S., Porterfield, D.M., Wei, A., Sepúlveda, M.S., 2011. Toxicological studies on silver nanoparticles: challenges and opportunities in assessment, monitoring and imaging. Nanomedicine 6 (5), 879–898, 10.2217/nnm.11.78. PMID: 21793678.
Takvam, M., Wood, C.M., Kryvi, H., Nilsen, T.O., 2021. Ion transporters and osmoregulation in the kidney of teleost fishes as a function of salinity. Front. Physiol. 12, 664588 https://doi.org/10.3389/fphys.2021.664588. PMID: 33967835 PMC8098666.
Tejamaya, M., Römer, I., Merrifield, R.C., Lead, J.R., 2012. Stability of citrate, PVP, and PEG coated silver nanoparticles in ecotoxicology media. Environ. Sci. Technol. 46 (13), 7011–7017. https://doi.org/10.1021/es2038596, 2012.
Tou, F., Wu, J., Fu, J., Niu, Z., Liu, M., Yang, Y., 2021. Titanium and zinc-containing nanoparticles in estuarine sediments: occurrence and their environmental implications. Sci. Total Environ. 754, 142388 https://doi.org/10.1016/j.scitotenv.2020.142388.
Tovar-Sanchez, A., Sanchez-Quiles, D., Basterretxea, G., Benede, J.L., Chisvert, A., Salvador, A., Moreno-Garrido, I., Blasco, J., 2013. Sunscreen products as emerging pollutants to coastal waters. PLoS One 8 (6), e65451.
Tucci, P., Porta, G., Agostini, M., Dinsdale, D., Iavicoli, I., Cain, K., Finazzi-Agró, A., Melino, G., Willis, A., 2013. Metabolic effects of TIO_2 nanoparticles, a common component of sunscreens and cosmetics, on human keratinocytes. Cell Death Dis. 4 (3), e549. https://doi.org/10.1038/cddis.2013.76.
Umair, M., Javed, I., Rehman, M., Madni, A., Javeed, A., Ghafoor, A., Ashraf, M., 2016 Apr-Jun. Nanotoxicity of inert materials: the case of gold, silver and iron. J. Pharm. Pharmaceut. Sci. 19 (2), 161–180, 10.18433/J31021. PMID: 27518167.
Vicari, T., Dagostim, A.C., Klingelfus, T., Galvan, G.L., Monteiro, P.S., da Silva Pereira, L., Silva de Assis, H.C., Cestari, M.M., 2018. Co-exposure to titanium dioxide nanoparticles ($NpTiO_2$) and lead at environmentally relevant concentrations in the Neotropical fish species Hoplias intermedius. Toxicol Rep 5, 1032–1043. https://doi.org/10.1016/j.toxrep.2018.09.001.
Vignardi, C.P., Hasue, F.M., Sartório, P.V., Cardoso, C.M., Machado, A.S., Passos, M.J., Santos, T.C., Nucci, J.M., Hewer, T.L., Watanabe, I.S., Gomes, V., Phan, N.V., 2015. Genotoxicity, potential cytotoxicity and cell uptake of titanium dioxide nanoparticles in the marine fish Trachinotus carolinus (Linnaeus, 1766). Aquat. Toxicol. 158, 218–229. https://doi.org/10.1016/j.aquatox.2014.11.008. PMID: 25481788.
Wang, J., Li, N., Zheng, L., Wang, S., Wang, Y., Zhao, X., Duan, Y., Cui, Y., Zhou, M., Cai, J., Gong, S., Wang, H., Hong, F., 2010. P38-Nrf-2 signaling pathway of oxidative stress in mice caused by nanoparticulate TiO_2. Biol. Trace Elem. Res. 140 (2), 186–197. https://doi.org/10.1007/s12011-010-8687-0. PMID: 20422311.
Wang, H., Ho, K.T., Scheckel, K.G., Wu, F., Cantwell, M.G.C., Katz, D.R., Horowitz, D.B., Boothman, W.S., Burgess, R.M., 2014. Toxicity, bioaccumulation, and biotransformation of silver nanoparticles in marine organisms. Environ. Sci. Technol. 48 (23), 13711–13717. https://doi.org/10.1021/es502976y.
Wani, M.R., Shadab, G., 2020. Titanium dioxide nanoparticle genotoxicity: a review of recent in vivo and in vitro studies. Toxicol. Ind. Health 36 (7), 514–530, 10.1177/0748233720936835. PMID: 32962563.
Williams, N.C., O'Neill, L.A.J., 2018 Feb 5. A role for the Krebs cycle intermediate citrate in metabolic reprogramming in innate immunity and inflammation. Front. Immunol. 9, 141. https://doi.org/10.3389/fimmu.2018.00141.
Wiśniewski, J., Zougman, A., Nagaraj, N., Mathias, M., 2009. Universal sample preparation method for proteome analysis. Nat. Methods 6, 359–362. https://doi.org/10.1038/nmeth.1322.
Wiśniewski, J.R., Ostasiewicz, P., Mann, M., 2011. High recovery FASP applied to the proteomic analysis of microdissected formalin fixed paraffin embedded cancer tissues retrieves known colon cancer markers. J. Proteome Res. 10, 3040–3049.
Wu, M., Guo, H., Liu, L., Liu, Y., Xie, L., 2019. Size-dependent cellular uptake and localization profiles of silver nanoparticles. Int. J. Nanomed. 14, 4247–4259. https://doi.org/10.2147/IJN.S201107.
Yin, I.X., Zhang, J., Zhao, I.S., Mei, M.L., Li, Q., Chu, C.H., 2020. The antibacterial mechanism of silver nanoparticles and its application in dentistry. Int. J. Nanomed. 15, 2555–2562. https://doi.org/10.2147/IJN.S246764.
Yue, Y., Li, X., Sigg, L., et al., 2017. Interaction of silver nanoparticles with algae and fish cells: a side by side comparison. J. Nanobiotechnol. 15, 16. https://doi.org/10.1186/s12951-017-0254-9.
Zhang, J., Guy, M.J., Norman, H.S., Chen, Y.C., Xu, Q., Dong, X., Guner, H., Wang, S., Kohmoto, T., Young, K.H., Moss, R.L., Ge, Y., 2011. Top-down quantitative proteomics identified phosphorylation of cardiac troponin I as a candidate biomarker for chronic heart failure. J. Proteome Res. 10 (9), 4054–4065. https://doi.org/10.1021/pr200258m.
Zhang, H., Yi, L., Sun, R., Zhou, H., Xu, W., Zhanga, W., Mai, K., 2016a. Effects of dietary citric acid on growth performance, mineral status and intestinal digestive enzyme activities of large yellow croaker Larimichthys crocea (Richardson, 1846) fed high plant protein diets. Aquaculture 453, 147–153. https://doi.org/10.1016/j.aquaculture.2015.11.032.
Zhang, X.F., Shen, W., Gurunathan, S., 2016b. Silver nanoparticle-mediated cellular responses in various cell lines: an in vitro model. In: Int J Mol Sci, vol. 17. PMCID, p. 1603. https://doi.org/10.3390/ijms17101603. PMID: 27669221.
Zhang, X., Smits, A.H., van Tilburg, G.B.A., Ovaa, H., Huber, W., Vermeulen, M., 2018. Proteome-wide identification of ubiquitin interactions using UbIA-MS. In: Nature Protocols, vol. 13, pp. 530–550.